Basin Research

WILEY

Basin Research IAS EAGE

RESEARCH ARTICLE OPEN ACCESS

Transport and Depositional Processes of Neogene Pumice Fragments in a Distal Fluvial System of the Northern Patagonian Foreland (Argentina)

Lucas Peñacorada[1] | Ricardo Gómez[2] | Maisa Tunik[1,3] | Silvio Casadio[4]

[1]Instituto de Investigación en Paleobiología y Geología, Universidad Nacional de Río Negro, General Roca, Río Negro, Argentina | [2]Géosciences Rennes, UMR 6118, CNRS Université de Rennes, Rennes, France | [3]Consejo Nacional de Investigaciones Científicas y Técnicas (CONICET), Buenos Aires, Argentina | [4]Facultad de Ingeniería, Geología, Universidad Andres Bello, Concepción, Chile

Correspondence: Lucas Peñacorada (lucaspenacorada@gmail.com)

Received: 30 May 2024 | **Revised:** 27 March 2025 | **Accepted:** 7 April 2025

Funding: This work was supported by Universidad Nacional de Río Negro and Consejo Nacional de Investigaciones Científicas y Técnicas.

Keywords: depositional processes | Miocene | northern Patagonia | pumice fragments

ABSTRACT

There are numerous studies analysing volcaniclastic supply to continental environments in distal areas from source volcanoes. However, there are few examples where large pumice fragments are mentioned in distal fluvial deposits. In this work, the Miocene synorogenic deposits of the Northern Patagonian Foreland (Chichinales and El Palo Formations) were studied. The deposits of the latter unit include pumice fragments with diameters of up to 30 cm that were accumulated in a fluvial environment more than 200 km from the Andean volcanic arc. Although previous works mention the presence of pumice in this unit, an analysis of the origin, the transport and depositional processes of these fragments was not carried out. Based on the study of stratigraphic sections along the extra-Andean zone, it was determined that the sediments of the Lower Miocene (Chichinales Formation) were deposited in a low-to-medium energy fluvial environment with development of wide floodplains and palaeosol formation during stability periods. The Middle Miocene?—Lower Pliocene deposits (El Palo Formation) correspond to a moderate-to-high energy braided fluvial system with occasional high discharge periods. The pumice fragments present in this unit were derived from the reworking of primary pyroclastic deposits outcropping at the foot of the Andes, associated with important explosive volcanic activity during the Miocene. These fragments were transported and deposited by both dilute flows and sediment gravity flows with high concentrations of pumice. Petrographic analysis of El Palo Formation sandstones showed a provenance mostly related to the erosion of pyroclastic, arc-related deposits. The main source areas would have been the Andean arc and the North Patagonian Massif. A maximum depositional age of 14.6 ± 1 Ma was obtained in a sample from the El Palo Formation, which constitutes the first U–Pb dating of detrital zircons from this unit in the study area. This age matches with a peak of magmatic activity of the Patagonian Batholith responsible for huge arc-derived ignimbrites recorded at the foot of the Andes.

1 | Introduction

Explosive volcanic activity provides significant volumes of pyroclastic material to sedimentary environments, both through primary input and subsequent remobilisation (Fisher and Schmincke 1984; Smith 1987). One of the most common products of large-scale explosive eruptions is vitroclast fragments with diverse granulometry, from ash to pumice lapilli. The latter consists of highly vesiculated volcanic glass fragments with variable composition (Fisher and Schmincke 1984). The term pumice has been used to describe various types of juvenile volcanic components, although in most cases, it refers to materials

Summary

- Neogene Northern Patagonian Basin.
- Distal volcaniclastic environment.
- Pumice fragments of up to 30 cm.

with a density lower than 1 g/cm^3 and the ability to float in water (Witham and Sparks 1986; Manville et al. 1998). Their low density allows them to be transported by river systems or marine currents over considerable distances until they are progressively saturated with water, changing their equivalent hydraulic radius and turning into bedload transport (Frick and Kent 1984; Mack et al. 1996; Bryan et al. 2012). Cold pumice clasts can maintain their buoyancy for days, months or even years, while those introduced into the water at high temperatures sink immediately (Witham and Sparks 1986). Additionally, experimental evidence has shown that larger fragments remain afloat for longer periods than smaller ones (Manville et al. 1998). Once they sink, pumice clasts are transported by common sedimentary processes, but their low density imparts unique hydrodynamic properties. The minimum energy required to mobilise them is lower than that for other similarly sized and denser clasts. Furthermore, these clasts remain in motion even at low flow velocities (Manville et al. 2002).

Numerous studies have been conducted to analyse the behaviour of pumice in fluvial, lacustrine and marine environments (Turbeville 1991; Manville et al. 1998, 2002; Jutzeler et al. 2015; Colombo et al. 2018; among others). However, there are few examples describing deposits with large-sized pumice fragments in distal continental environments (> 100 km) from the source (e.g., Mack et al. 1996; Kataoka 2003). This study presents an example of Miocene continental deposits rich in pumice clasts, with diameters of up to 30 cm, accumulated in a fluvial environment over 200 km away from the Andean volcanic arc. The El Palo Formation (Middle Miocene?—Lower Pliocene) is exposed in the area between the Negro and Colorado rivers (Figure 1a–c), which has been described by various authors within the framework of regional geological studies (Hugo and Leanza 2001a; Rodríguez et al. 2023). Although the literature briefly mentions the presence of pyroclastic material and reworked pumice fragments, no studies have focused on their transport and deposition processes.

The objectives of this study were to refine the paleoenvironmental model, delineate the sediment source area and elucidate the transport and deposition mechanisms of the pumice fragments. Additionally, despite a previous background that indicates an Upper Miocene to Lower Pliocene age for the unit and its equivalents based on paleontological content (Alberdi et al. 1997), this study presents the first data of U–Pb detrital zircon analysis from a sample of the El Palo Formation.

2 | Background

The Chichinales Formation was formally defined by Fossa Mancini et al. (1938) and overlies unconformably Upper Cretaceous–Paleogene deposits (Neuquén and Malargüe groups). It is composed of yellowish-brown to yellowish and greenish-grey conglomerates, volcaniclastic sandstones, mudstones and tuffs (Uliana 1979; Barrio et al. 1989; Hugo and Leanza 2001a; Rodríguez et al. 2023). These authors interpreted a continental environment for this area, characterised by alternating deposits of fluvial channel fills, floodplain deposits and aeolian accumulations.

Regarding the age of the unit, previous studies suggested a Lower Oligocene–Middle Miocene age, based on fossil mammals (Pascual and Bondesio 1985; Barrio et al. 1989; Hugo and Leanza 2001a). Recently, an age of 20.49 ± 0.05 Ma (^{40}Ar/^{39}Ar) was obtained from a tuff bed in the upper section of this unit within the study area (Rodríguez et al. 2023).

The El Palo Formation, originally defined by Uliana (1979), comprises a set of grey-blue sandstones. Stratigraphically, it is positioned below the Chichinales and Los Loros formations and is overlain by the Bayo Mesa Formation. According to Uliana (1979), the El Palo Formation was deposited in an anastomosed fluvial environment with varying energy, featuring fine intercalations with calcareous concretions and palaeosols corresponding to alluvial plains.

Concerning the age of the unit, the fossil mammals, initially attributed to the Río Negro Formation and later correlated with the El Palo Formation, suggest an upper Miocene–lower Pliocene age (Scillato Yané et al. 1975; Pascual et al. 1984; Pascual and Bondesio 1985; Alberdi et al. 1997).

3 | Geotectonic Framework

Numerous studies have analysed the changes in the tectonic regime of the Andes and their influence on the evolution of Cenozoic sedimentary basins after the infilling of the Neuquén Basin, primarily in sectors near the orogenic front (e.g., Franzese et al. 2011; Huyghe et al. 2014; López et al. 2019). During the Middle-to-Late Miocene, syncontractional deposition of forearc strata occurred through the inversion of basement faults located west of the study area. This process was contemporaneous with the development of the retroarc fold-thrust belt and the onset of intraplate contraction, which began around 18–16 Ma in the axial Cordilleran zone and propagated eastward between approximately 15–9 Ma, leading to the formation of foreland basins (Echaurren et al. 2022 and references therein). The contractional regime facilitated the evolution and growth of the Patagonian Broken Foreland System, characterised by well-studied depocenters. Associated volcanism during this period imparted a distinct compositional signature to the alluvial-fluvial systems (Bilmes et al. 2013; Orts et al. 2012; Franzese et al. 2018; López et al. 2019; D'Elia et al. 2020). Additionally, the establishment of orographic rain shadows emerged as a critical process in the Patagonian Andes, significantly influencing regional climate patterns (Ortiz-Jaureguizar and Cladera 2006; Bucher et al. 2020).

While regional tectonic subsidence is widely regarded as the primary control on accommodation space and sediment supply in foreland basin systems (e.g., Schumm 2005; Huerta et al. 2011), both tectonic and climatic processes played pivotal roles in shaping the Neogene alluvial-fluvial systems of northern Patagonia (Bilmes et al. 2013; Bucher et al. 2020; López et al. 2019, 2024; García Morabito et al. 2021). The interplay of these factors exerted

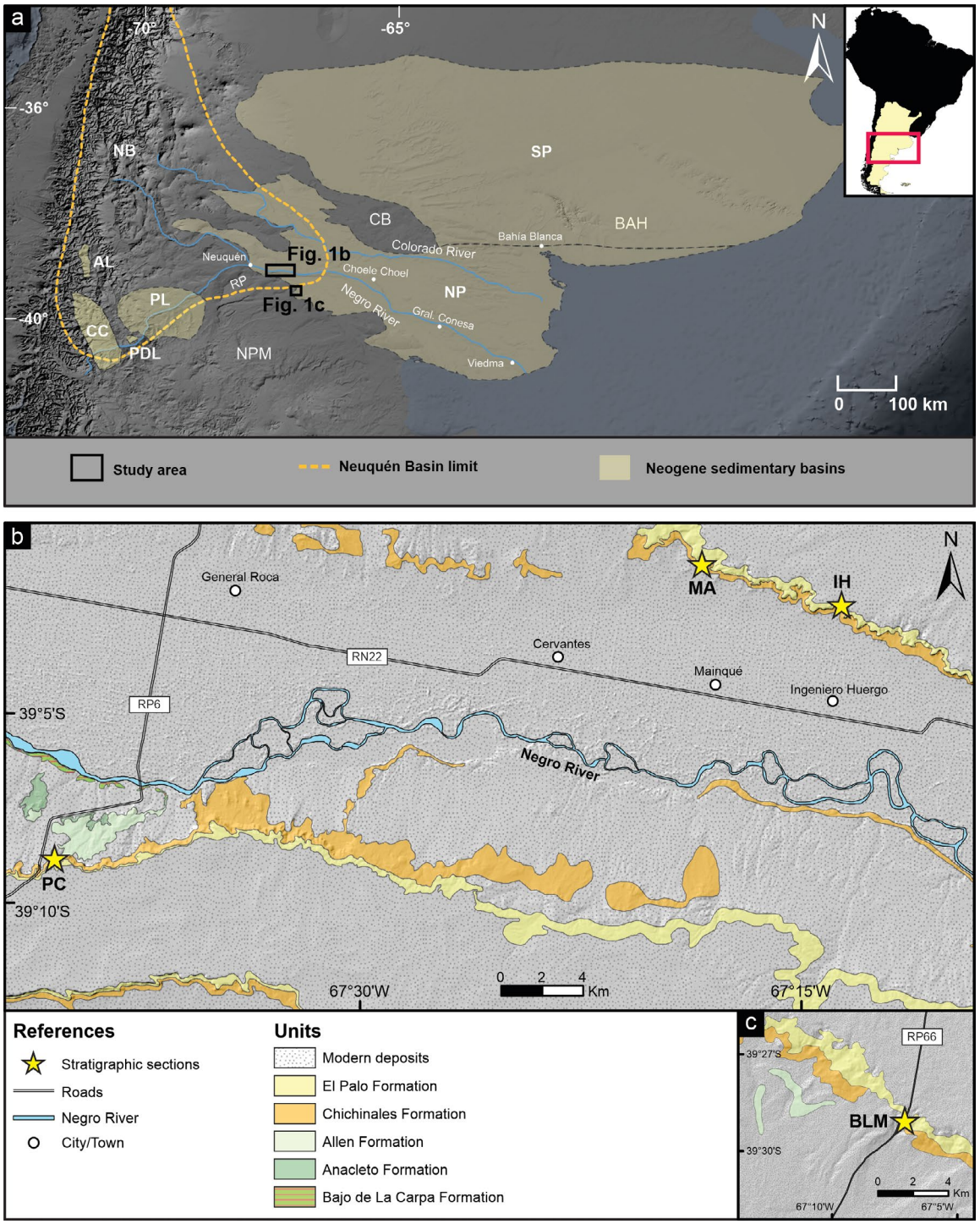

FIGURE 1 | (a) Location of the main regional geotectonic features. Black rectangles indicate the study areas. CB, Chadileuvú Block; NB, Neuquén Basin; NP, North Patagonian Basin (according to Folguera et al. 2015); BAH, Buenos Aires High; NPM, North Patagonian Massif. (b) Geological map of the Alto Valle area near Negro River. (c) Geological map of the Bajo Los Menucos area. The yellow stars indicate the location of stratigraphic sections. BLM, Bajo Los Menucos; IH, Ingeniero Huergo; MA, Mainqué; PC, Paso Córdoba.

a long-term influence on the sedimentary environments preserved in the Miocene deposits of Northern Patagonia.

In the central extra-Andean sector of Argentina, studies have linked Cenozoic Andean tectonics with sedimentation in the distal foreland (Folguera and Zárate 2009; Folguera 2011; Folguera et al. 2015). Based on the distribution of deposits and depocenter geometry, these authors identified two Neogene extra-Andean foreland basins, known as the Southern Pampa Basin and the North Patagonian Basin (Figure 1a). The latter is limited to the north by the Chadileuvú Block and the Bonaerense High, and to the south by the North Patagonian Massif, extending approximately from eastern Neuquén Province to the Atlantic coast. The infill of this basin consists of recurrent Neogene

sedimentation cycles, including the Rentería, Barranca de los Loros, El Palo, Bayo Mesa, El Sauzal and Río Negro formations (Folguera et al. 2015). In the area of this study, located in the southwestern sector of the North Patagonian Basin, only the deposits of the El Palo Formation are exposed.

4 | Materials and Methods

The geological map was carried out using GIS software, based on satellite images from the United States Geological Survey (USGS), and overlaying the geological maps of General Roca (3969-IV) and Villa Regina (3966-III).

The survey of stratigraphic sections involved measuring thicknesses using a Jacob's staff, recording detailed descriptions of the textural characteristics of the recognised facies, identifying layer geometries and systematically collecting representative samples. Measurements of strike, dip and paleocurrent directions were performed using a Brunton compass.

We selected 13 samples for the preparation of 30 μm thin sections. They were impregnated with blue epoxy resin to enhance porosity and were stained with alizarin red and potassium ferricyanide, following Dickson (1966a, 1966b) method for carbonate differentiation. Subsequently, five thin sections were chosen for modal analysis, which was performed using a point-counting stage and associated software. The remaining thin sections were described and classified, as they did not meet the criteria for modal analysis due to their very fine lithologies, matrix content exceeding 15%, or the presence of abundant poikilotopic cement. The sandstones were classified based on Garzanti (2019) diagram, and modal counting was carried out using the Gazzi–Dickinson method, with 400 points counted in each thin section (Ingersoll et al. 1984). The results were plotted on Dickinson et al. (1983) provenance diagrams.

The petrographic study was complemented by analysing sample 'IH05' using a ZEISS EVO MA15 scanning electron microscope (SEM). Additionally, sample 'PPC01-20' was processed to obtain U–Pb ages in detrital zircons in two stages: the first was carried out at the Instituto de Investigación en Paleobiología y Geología (IIPG) and included milling in a widia jaw crusher and separation of the material into different grain sizes with the use of a mechanical sieve shaker and a set of sieves with different graduations. Subsequently, as the second stage, fractions retained in the 500 and 250 μm sieves were sent to the La.Te. Andes S.A. laboratory, where zircon separation was initially performed using heavy liquids and an isodynamic magnetic separator. Zircon grains were then analysed at the laboratory using a Laser Ablation Inductively Coupled Plasma Mass Spectrometer (LA-ICP-MS).

5 | Results

5.1 | Facies Analysis

The four sedimentary sections surveyed between the localities of General Roca and Bajo Los Menucos include the Chichinales and El Palo formations (Figure 2). Eleven sedimentary facies were identified and interpreted, summarised in Table 1. These were grouped into four facies associations: Floodplain (FA1), Isolated Sandy Channels (FA2), Amalgamated Gravelly-Sandy Channels (FA3) and Sheet Flows Deposits (FA4).

The contact between Chichinales and El Palo formations is erosive, except in the Bajo Los Menucos section, where it was observed as transitional. Differences in particle size and composition can also be noted between these units. The Chichinales Formation is dominated by deposits of FA1 and FA2, composed of coarse to fine sandstones and mudstones, while the El Palo Formation is characterised by conglomerates and coarse to fine sandstones included in FA3 and FA4. In this latter unit, fine deposits of FA1 are poorly represented or spatially restricted.

5.1.1 | Facies Association 1 (FA1)—Floodplain

This facies association is dominant in the lower part of the surveyed sections, while it becomes less represented or spatially restricted towards the upper part. It is composed of tabular beds of laminated or massive mudstones (Facies Fl and Fm; Figure 3a,b), interbedded with thin bodies of coarse to fine sandstones exhibiting tabular, small-scale lenticular or irregular geometries, with parallel, ripple or massive lamination (Facies Sfh, Sm and Sr.; Figure 3c–e). The presence of iron and manganese oxide nodules, rhizoliths and undifferentiated bioturbation in the form of vertical and horizontal tubes is common (Figure 3d). The clasts mainly consist of quartz, feldspars and angular to subangular cuspate and pumiceous shards. The proportion of these latter components varies, being dominant in some beds and completely absent in others.

5.1.1.1 | Interpretation. The tabular beds of fine sandstone facies and massive or laminated mudstones were interpreted as the result of suspension load fall-out processes in fluvial floodplains. The sandstones with erosional bases and tabular, small-scale lenticular or irregular geometries correspond to crevasse deposits associated with flood events (Miall 1996). Sets with fine-grained texture, mainly composed of volcaniclastic glassy components, represent reworked deposits of volcanic ashfall (Smith 1987). The presence of mial rhizoliths and undifferentiated bioturbation indicates colonisation by organisms during periods of stability, while the manganese and iron nodules are associated with the remobilisation of these elements during wet periods and their subsequent precipitation during dry seasons (PiPujol and Buurman 1997).

5.1.2 | Facies Association 2 (FA2)—Isolated Sandy Channels

This association is almost entirely restricted to the lower sector of the surveyed sections. It consists of lenticular or tabular sandy bodies with erosional bases, and individual thicknesses generally not exceeding 3 m. In most cases, these bodies are isolated or weakly amalgamated and surrounded by deposits of FA1 (Figure 4). Internally, they display planar and trough cross-stratification, parallel lamination, normal grading or may be massive (Facies St, Sh, Sm; Figure 4b,c), and commonly exhibit rhizoliths and ripple lamination towards the top (Facies Sr.; Figure 4b). Additionally, common large-scale lateral accretion structures were observed in the Bajo Los Menucos section (Figure 4d).

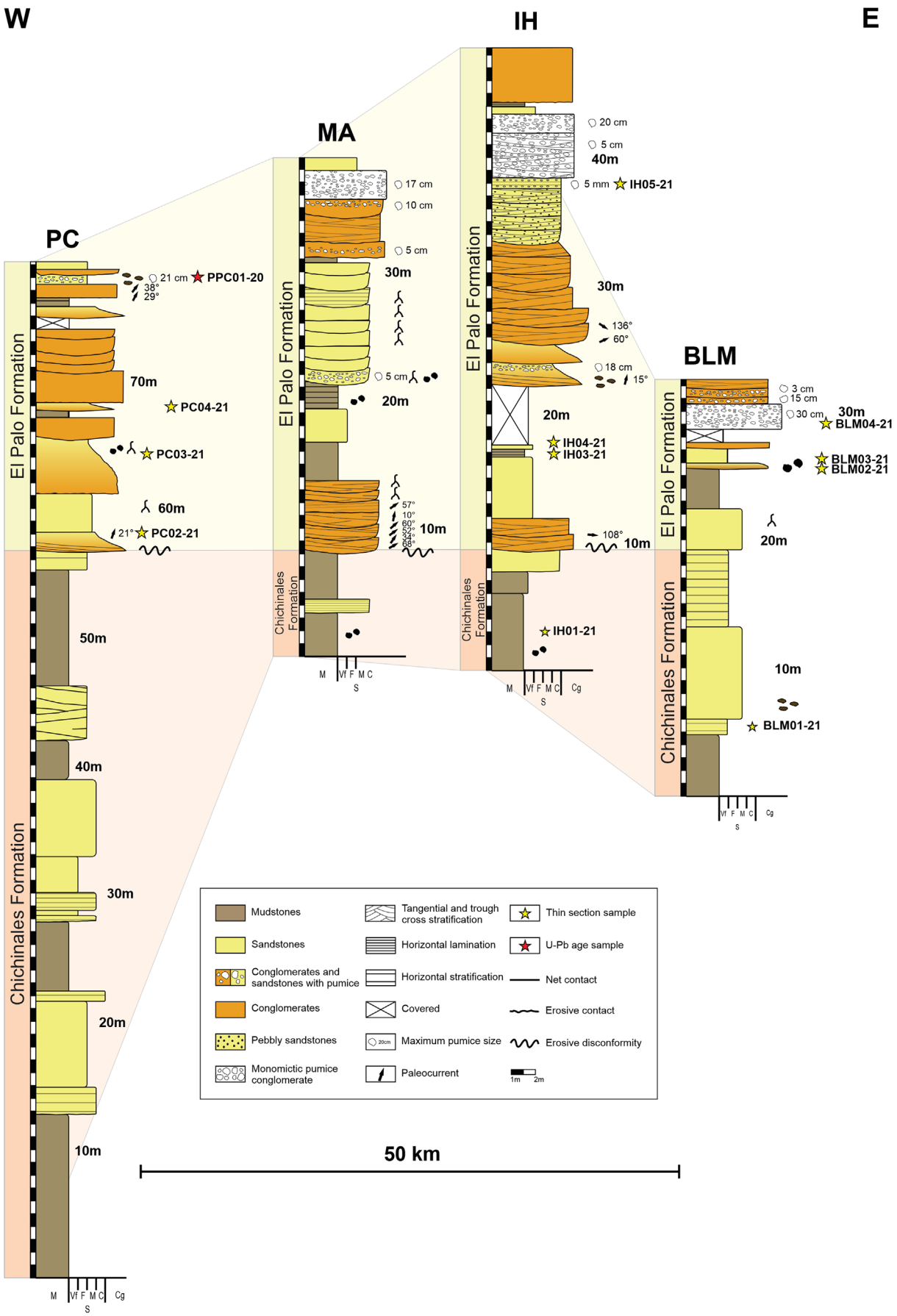

FIGURE 2 | Stratigraphic sections of the Chichinales and El Palo formations in the Paso Córdoba (PC), Mainqué (MA), Ingeniero Huergo (IH), and Bajo Los Menucos (BLM) areas.

TABLE 1 | Code, description and interpretation of the defined sedimentary lithofacies. Codes were taken and modified from Miall (1996).

Code	Description	Interpretetation	Comments
Gcm	Clast-supported conglomerates, massive or normal graded, in lenticular or tabular beds. Erosive base	Bedload in channel bodies	Frequent intraclasts at the base
Gmm	Matrix-supported conglomerates, massive or with diffuse stratification and moderate to poor sorting, with tabular or irregular geometries	Gravity flows	Frequently exhibit abundant lapilli and block-sized pumice
Gh	Clast-supported conglomerates with parallel stratification, in lenticular or tabular beds. Erosive base	Longitudinal bedforms or lag deposits	—
Gt	Clast-supported conglomerates with tangential cross-bedding and trough cross-stratification, in lenticular or tabular beds. Erosive base	Bedform migration in channel bodies	Occasional intraclasts at the base
St	Fine to coarse-grained or pebbly sandstones with tangential cross-bedding and trough cross-stratification, in lenticular or tabular beds. Erosive base	Bedform migration in channel bodies	—
Sm	Massive, fine to coarse-grained or pebbly sandstones, in tabular beds and to a lesser extent, lenticular beds	Rapid deposition by sediment-laden flows or massive deposits due to bioturbation	Frequent rhizoliths, undifferentiated bioturbation and mottles/nodules
Sh	Fine to coarse-grained sandstones with horizontal lamination or bedding, in tabular or occasionally lenticular beds. Sharp flat or slightly erosive base	Hyperconcentrated flows or sheet flows	May contain pumice not exceeding 5 mm, concentrated in layers
Sr	Fine to medium-grained sandstones with ripple lamination	Current ripples in low-regime flows	—
Sfh	Fine-grained sandstones with parallel lamination, in tabular beds. Flat base	Sediment settling in shallow bodies of water	—
Fl	Mudstones with horizontal lamination or bedding in tabular beds. Flat base	Sediment settling in shallow bodies of water	—
Fm	Massive mudstones in tabular beds. Flat base	Sediment settling in shallow bodies of water	Frequent undifferentiated bioturbation and mottles/nodules

Regarding the composition, these deposits generally have a high proportion of quartz and subordinate pyroclastic material.

5.1.2.1 | **Interpretation.** The lenticular and tabular sandy deposits with erosional bases correspond to fluvial channels. The presence of planar and trough cross-stratification structures indicates the migration of bedforms, while the ripple lamination at the top of the bodies was formed during deceleration stages under low-regime flow conditions. The development of bioturbation and palaeosols is associated with periods of stability or nondeposition (Bridge 2003). The sediment grain size and frequent interbedding with FA1 deposits suggest a system of low to moderate energy. In the Bajo Los Menucos locality, the recurrence of lateral accretion structures indicates the development of highly sinuous channels (Miall 1996), at least in that area.

5.1.3 | Facies Association 3 (FA3)—Amalgamated Gravelly-Sandy Channels

This facies association dominates the top of the measured sections. The deposits consist of clast-supported conglomerate facies and gravelly sandstones (Gt, Gh, Gcm, SGm, SGh, St, Sh, Sm), arranged in beds with erosional bases and lenticular or tabular geometries (Figures 5 and 6). These beds have individual thicknesses ranging from 0.5 to 2 m and are generally multiepisodic deposits bounded by erosional surfaces (Figures 5 and 6). At the bottom, intraclasts of fine sandstones or volcaniclastic mudstones are commonly observed, with diameters ranging from a few mm to 50 cm (Figure 5b). Occasionally, towards the top of the bodies, massive sandstones with abundant rhizoliths and incipient paedogenic structures are present (Figure 5c). Paleocurrent measurements from

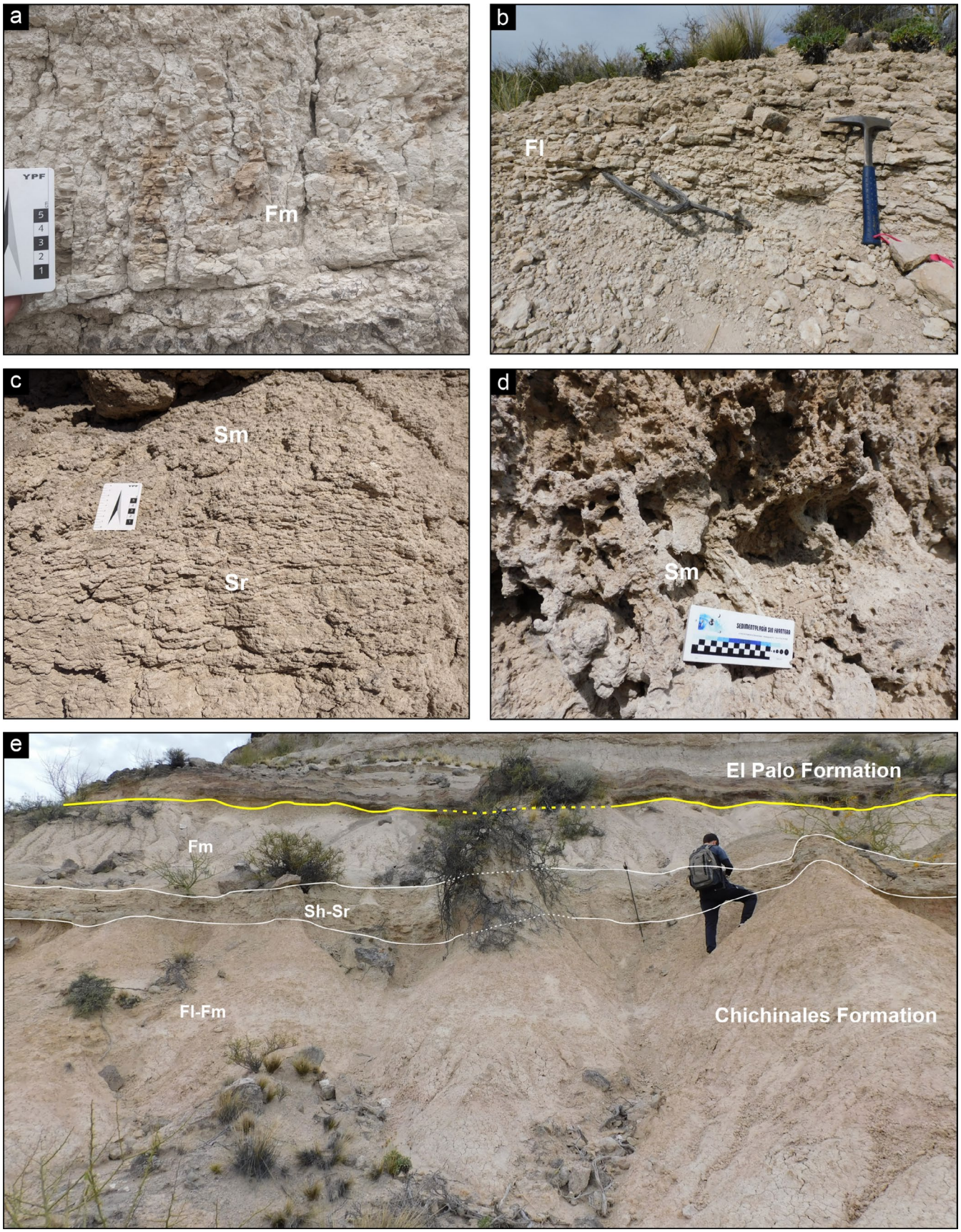

FIGURE 3 | Facies association 1. (a) Massive mudstones (Fm) with reddish mottling. (b) Tabular beds of mudstones with parallel lamination (Fl). (c) Ripple-laminated (Sr) and massive (Sm) sandstones. (d) Massive sandstones (Sm) with intense bioturbation by rhizoliths and undifferentiated fossil traces. (e) Tabular beds of sandstones with parallel and ripple lamination (Sh and Sr) between massive and laminated mudstone deposits (Fl and Fm), below the contact with the El Palo Formation.

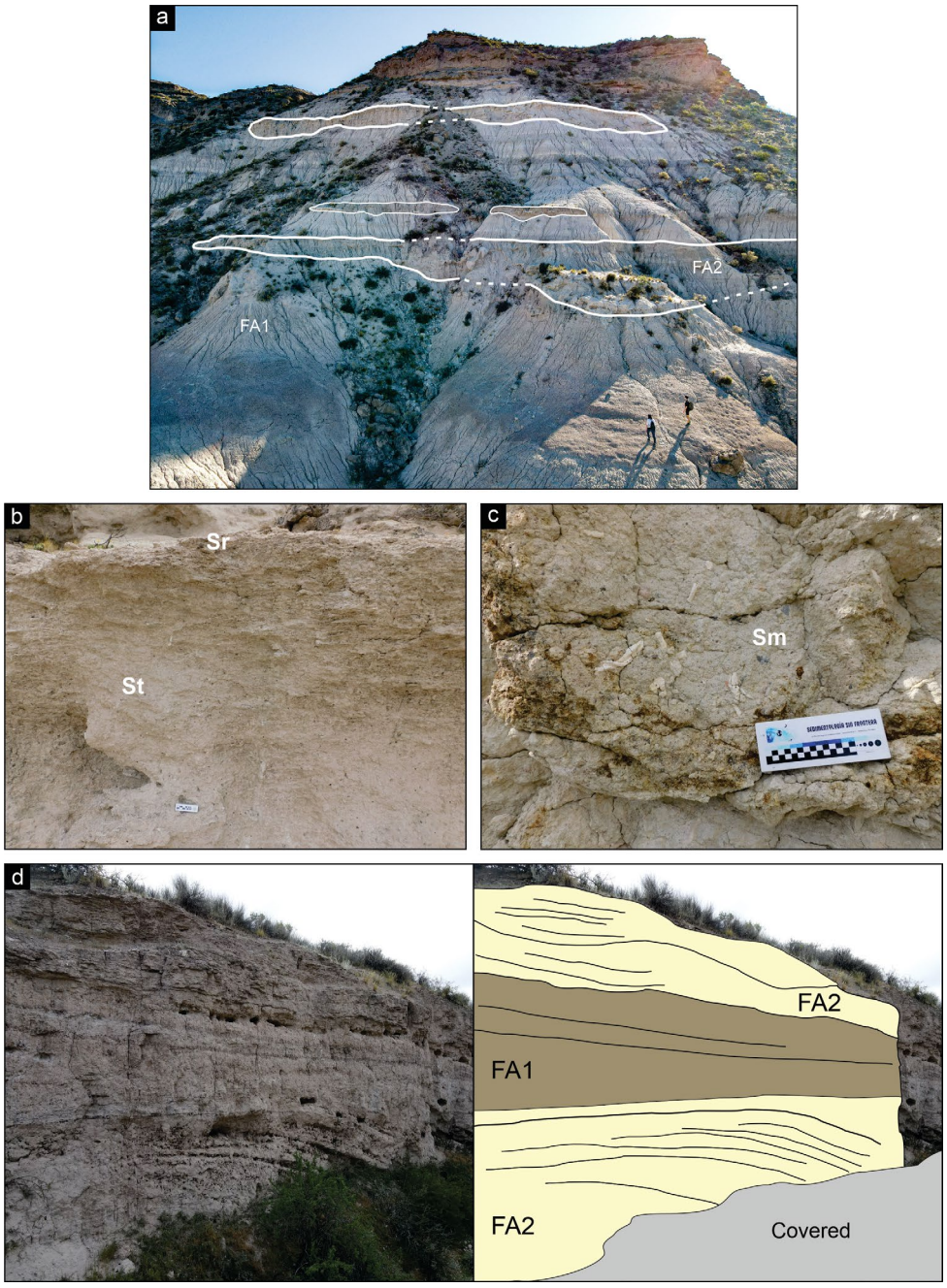

FIGURE 4 | Chichinales Formation Deposits. (a) Channelised bodies of FA2 isolated between fine-grained tabular deposits of FA1. (b) Sandstones with incipient tangential cross-stratification (St) and current ripples (Sr). (c) Massive sandstones (Sm) with rizoconcretions and reddish mottling in a lenticular bed. (d) Redrawing of the contact between FA1 and FA2 deposits. The body at the bottom of the image shows lateral accretion structures.

cross-stratification structures and imbricated clasts indicate a dominant palaeoflow direction towards the NE. In the Mainqué section, these palaeoflow directions are approximately parallel to the macroforms direction of accretion.

The clast composition is predominantly volcanic lithic, with variable proportions of epiclastic sediments of intermediate to basic composition and volcaniclastics mainly composed of vitroclasts. The pyroclastic material increases in abundance and size in the last 10 m of the surveyed sections, forming levels of mixed or even monomictic composition (Figure 5d). These consist mainly of pumice clasts ranging from ash to lapilli size, occasionally including larger block-sized fragments up to 18 cm. In all cases, the pumice clasts have a larger average size compared to sediments of other compositions deposited together (Figure 5e,f).

5.1.3.1 | **Interpretation.** The sedimentary deposits dominated by conglomerate clast-supported and stratified or massive sandstones in amalgamated lenticular bodies correspond to the infilling of gravel-bed channels in a fluvial system (Miall 1996). Although the grain size varies along the stratigraphic sections, the prevalence of gravels and gravelly sandstones, as well as the development of multiepisodic channels bounded

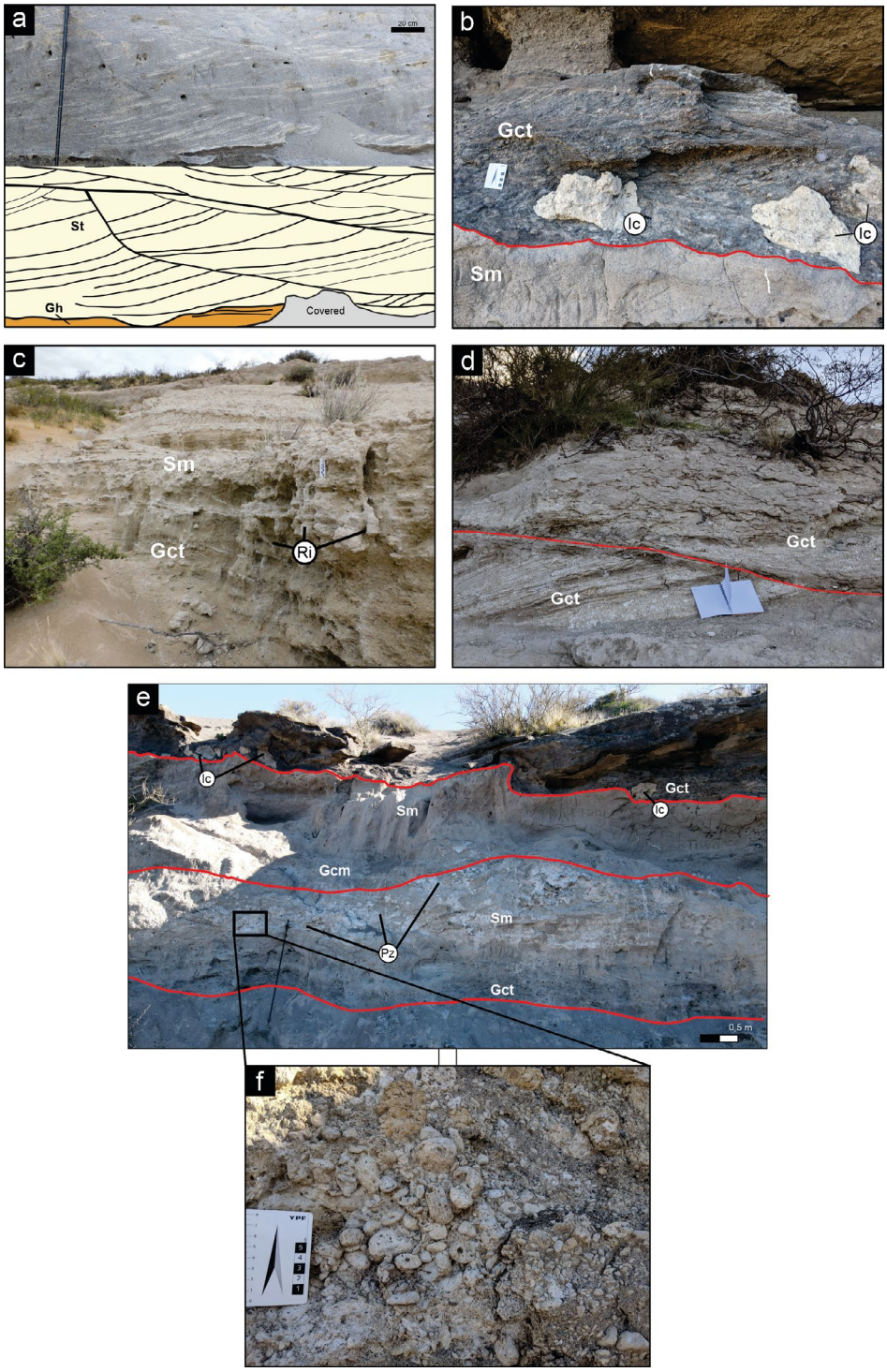

FIGURE 5 | Facies Association 3. (a) Redrawing of pebbly/gravelly sandstones with trough cross-stratification (St) overlying parallel-stratified conglomerates (Gh). (b) Trough and tangential cross-stratified conglomerates (Gct) in lenticular beds, over massive sandstones (Sm). On/At the base, volcaniclastic sand and mud intraclasts (Ic) can be observed. (c) Trough cross-stratified conglomerates (Gct) at the base of a channelised body. Towards the top, massive sandstones (Sm) and rizoliths (Ri) are visible. (d) Lenticular beds composed of apparently monomictic pumice conglomerates with cross-stratification (Gct). (e) Detail of a pumice fragment accumulation at the top of a fluvial bar. (f) Bar and channel deposits in the El Palo Formation. Ic, intraclasts; Pz, pumice.

by erosional surfaces, indicates conditions of moderate to high energy and high mobility channels (Gibling 2006). The abundance of intraclasts of various sizes, mainly composed of mudstones and fine sandstones, could indicate the incipient development and subsequent erosion of adjacent floodplain deposits or the reworking of previous volcaniclastic deposits. The occasional presence of fine grain sizes, current ripples and paedogenic features towards the top of some bodies

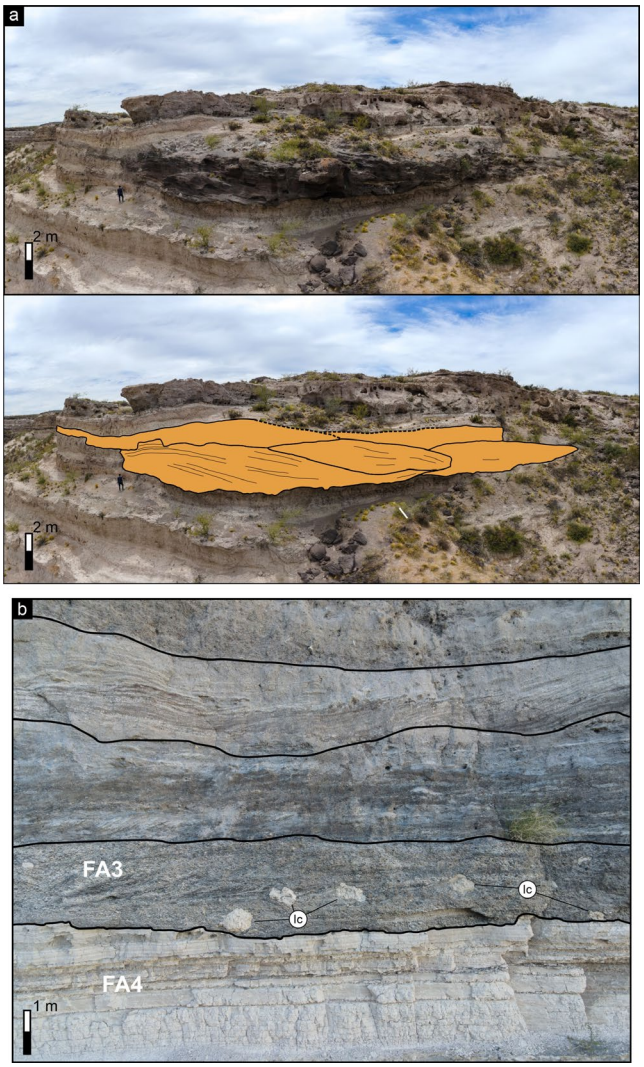

FIGURE 6 | (a) Redrawing of amalgamated gravelly channels of FA3. Ic, intraclasts. (b) Contact between tabular deposits of FA4 and conglomerate beds of FA3.

represents channel abandonment and avulsion events (Leddy et al. 1993). The direction of accretion of macroforms approximately parallel to the palaeoflow measured in the Mainqué area indicates the dominance of downstream accretion surfaces in low-sinuosity channels (Miall 1996), at least for this area. Regarding the pumice fragments in FA3, their origin corresponds to the fluvial reworking of primary pyroclastic deposits located at the catchment areas of the fluvial network or the erosion of previous deposits from FA4. The larger size of the pumice clasts compared to those of other compositions is due to their hydraulic equivalence with smaller denser clasts (Manville et al. 2002).

5.1.4 | Facies Association 4 (FA4)—Sheet Flow Deposits

The FA4 facies association is mainly composed of conglomerates and sandstones in sets that do not exceed 2 m in thickness, primarily tabular or irregular, and to a lesser extent lenticular. The conglomerates typically have a sandy matrix and are generally massive, although some areas show evidence of stratification or diffuse stratification (Gmm facies; Figure 5a–c). Large pumice fragments are abundant, occasionally forming monomictic beds, with diameters ranging from a few millimetres to exceptionally 20–30 cm. In the epiclastic fraction, clasts do not usually exceed 2 cm in diameter. Larger pumice clasts are commonly concentrated in clast-supported horizontal levels, although they can also occur isolated among other smaller-grained clasts (Figure 7c). Occasionally, subvertical orientations of pumice clasts are observed (Figure 7a). To a lesser extent, banks of matrix-supported conglomerates (Gmm facies) without pyroclastic material were identified.

The sandstones are coarse to fine and occur in massive or parallel laminations sedimentary structures (Facies Sm, Sh; Figure 7d,e). In the latter, sectors with laminations composed almost entirely of pumice fragments of a few millimetres were observed (Figure 7e). Occasionally, small ripples were observed towards the top of the laminated sandstones (Facies Sr.; Figure 7e). The conglomerate and sandstone bodies of FA4 are generally confined by deposits of FA3, although vertical amalgamation was observed (Figure 7d).

5.1.4.1 | Interpretation. The massive or diffusely stratified conglomerates and sandstones with poorly sorted clasts are characteristic of sediment gravity flows (Miall 1996). Considering the sandy matrix, grain size and presence of diffuse lamination or stratification, the conglomerates likely represent hyperconcentrated flows. The nearly monomictic beds with accumulations of large-sized pumice fragments are common towards the top of these deposits (Vallance and Iverson 2015). The tabular or sheet-flood deposits of coarse to medium laminated sandstones are interpreted as deposits from unconfined flash floods. The presence of ripples at the top of these bodies indicates flow deceleration (Miall 1996).

6 | Petrography

The thin sections analysed correspond to samples from the El Palo Formation, with the exception of samples IH01 and BLM01, which were collected from the top of the Chichinales Formation. Based on the modal analysis of five sandstones from the El Palo Formation (Table S1, Supporting Information S1) and using the diagram by Garzanti (2019), it was determined that the samples represent quartzo-feldspatho-lithic (PC02) and feldspatho-quartzo-lithic (PC03, PC04, PC05A and IH05) sandstones (Figure 8a). Using the QFL diagram by Dickinson et al. (1983), a dissected arc provenance is observed for samples PC02 and PC03, transitional arc for PC04 and PC05A, and undissected arc for sample IH05 (Table S2, Supporting Information S1; Figure 8b). The QmFLt diagram shows a mixed provenance for sample PC03, transitional arc for PC02 and PC05A, and lithic recycled for samples PC04 and IH05 (Table S3, Supporting Information S1; Figure 8b).

The remaining thin sections did not meet the conditions for modal analysis. Samples IH01 and IH03 correspond to limolites with abundant volcanic glass, while sample BLM01 is a fine to very fine sandstone mainly composed of pumice and cuspate vitroclasts, with subordinate amounts of quartz, feldspars and scarce epiclastic lithic fragments. Samples IH04,

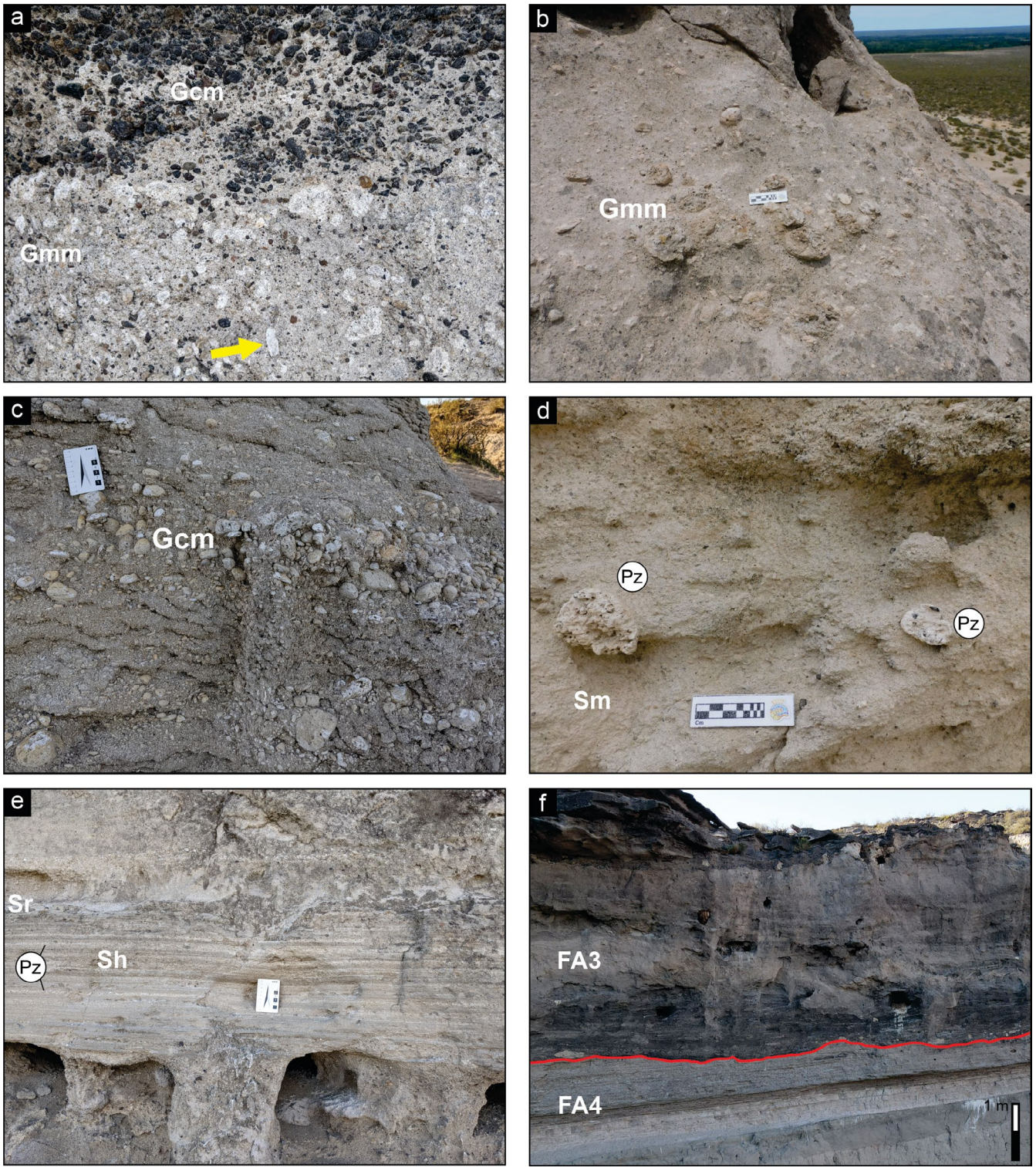

FIGURE 7 | Facies association 4. (a) Contact between massive conglomerates with pumice (Gmm) of FA4 and clast-supported conglomerates (Gcm) of FA3. The yellow arrow points to a vertically oriented pumice clast. (b) Massive conglomerate (Gmm) with numerous large pumice clasts. (c) Apparently monomictic pumice conglomerates with diffuse stratification (Gmm). Accumulations of lapilli and block-sized pumice are observed in horizontal levels. (d) Massive sandstones (Sm) with lapilli-sized pumice clasts (Pz). (e) Transition between sandstones with parallel lamination (Sh), ripple marks (Sr) and massive beds (Sm) at the top. At the bottom, layers composed almost entirely of pumice clasts (Pz) up to 2 mm in size can be seen. (f) Contact between tabular beds of laminated sandstones of FA4 and channelised gravel deposits of FA3.

PC05B, BLM02 and BLM03 are sandstones primarily composed of lithic fragments. These fragments are mostly of volcanic origin and have both volcaniclastic and epiclastic composition. They also contain quartz, plagioclases and, to a lesser extent, alkaline feldspars. Sample BLM04 corresponds to a pumice fragment.

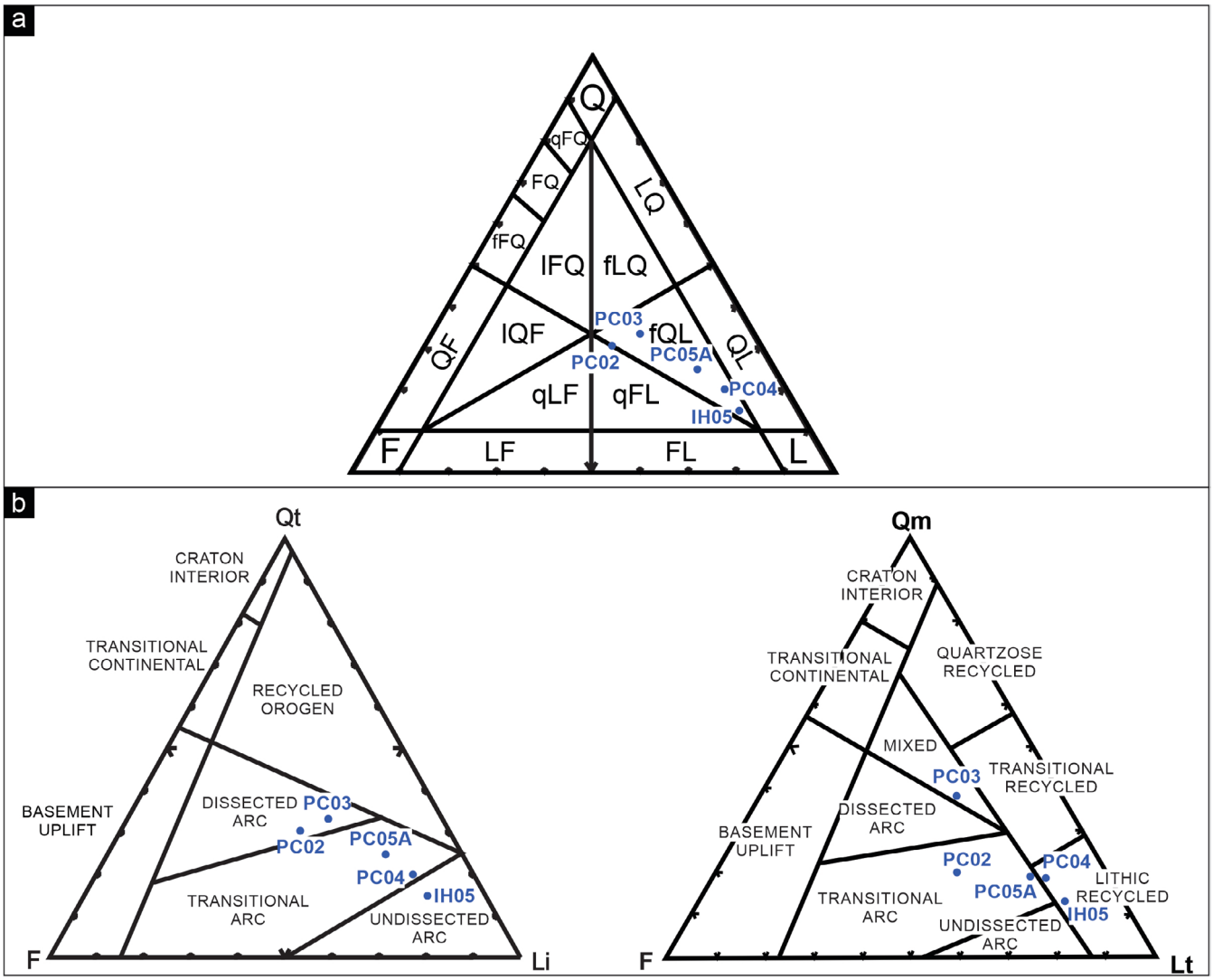

FIGURE 8 | Plot of the samples from El Palo Formation on the diagrams of (a) Garzanti (2019) and (b) Dickinson et al. (1983). F, feldspathic; FL, feldspatho-lithic; fLQ, feldspatho-litho-quartzose; FQ, feldspatho-quartzose (fFQ, feldspar-rich; qFQ, quartz-rich); fQL, feldspatho-quartzo-lithic; L, lithic; LF, litho-feldspathic; lFQ, litho-feldspatho-quartzose; LQ, litho-quartzose; lQF, litho-quartzo-feldspathic; Q, quartzose (qQ, pure quartzose); QF, quartzo-feldspathic; qFL, uartzo-feldspatho-lithic; QL, quartzo-lithic; qLF, quartzo-litho-feldspathic.

6.1 | Description of the Main Components

The quartz grains are present as subrounded to subangular fragments (Figure 9a,b). The most abundant type of quartz is monocrystalline with flash extinction (10% of the total), although varieties of monocrystalline with undulous extinction (5%) and polycrystalline (4%) were also identified, which, in some cases, are oriented parallel.

Among the feldspars, plagioclase is predominant compared to alkali feldspars (12% and 2% of the total, respectively). Individual plagioclase fragments are mostly subangular and exhibit polysynthetic twinning, very frequent zoning, and in some cases, they are weakly altered (Figure 9c). Plagioclase is also commonly found as phenocrysts or in the matrix of palaeovolcanic lithic fragments with lathwork and pilotaxic textures. Alkali feldspars are present as subrounded clasts and are generally altered by sericite or clay minerals (Figure 9c); occasionally, they show Carlsbad twinning and microperthitic textures.

The lithic fragments constitute the most abundant component in the analysed samples (44% of the total) and are predominantly composed of volcanic vitric acid lithics (21%) and mafic volcanic lithics fragments (10%). The former are represented by individual angular shards, pumice and pyroclastic lithics (Figure 9d–f). Pumice clasts can be locally very abundant (e.g., 19% in sample IH05), and the larger ones may contain internally oriented crystals of plagioclase, quartz and alkali feldspar. Their vesicles are often observed to be coated with an opaque material composed of clays (Figure 9d). In some cases, the vesicles are filled with carbonates. The mafic volcanic clasts show pilotaxitic and lathwork textures, where the main components are aligned plagioclase crystals (Figure 10a). Sedimentary lithic fragments are present in low proportions in samples PC02, PC05A and IH05 (< 5%), while in samples PC03 and PC04, they represent 15% and 35% respectively. In most cases, these clasts correspond to fine volcaniclastic deposits (Figure 10b). In smaller proportions, volcanic lithic fragments with granular and seriate textures (2%), oriented metamorphic lithic fragments (< 1%) and plutonic lithic

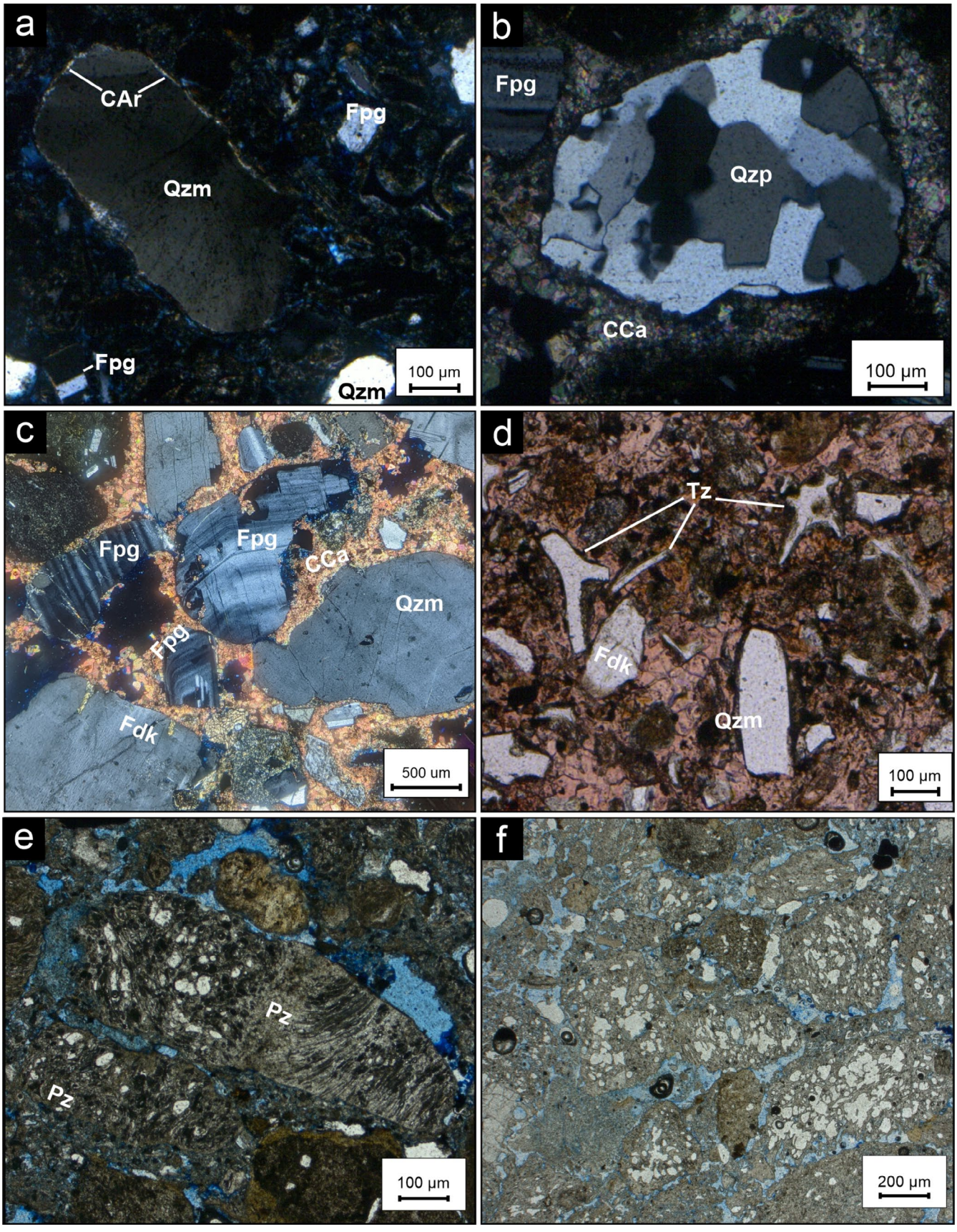

FIGURE 9 | Legend on next page.

FIGURE 9 | Microphotographs of thin sections of the El Palo Formation. (a) Monocrystalline quartz with undulose extinction (Qzm), plagioclase (Fpg) and argillaceous cement filling pores (CAr). (b) Polycrystalline quartz grain with more than three components (Qzp), surrounded by calcareous cement (CCa). (c) Clasts of plagioclase with concentric zoning and polysynthetic twinning (Fpg), monocrystalline quartz (Qzm), and potassium feldspar (Fdk). (d) Angular glass shards (Tz), potassium feldspar (Fdk) and monocrystalline quartz (Qzm). (e) Pumice clasts (Pz) with vesicles partially coated by clays. (f) Pumice clasts with uncoated vesicles.

fragments (< 1%) were identified, including quartz with graphic texture and perthitic K-feldspars (Figure 10c).

The abundance of pyroxenes is notable in sample PC02 (17%), obtained at the bottom of the El Palo Formation in the Paso Córdoba area. They show inclusions of opaque minerals and are frequently fractured (Figure 10d). They are predominantly found as individual subrounded to subangular crystals, although they can also be present as part of the matrix of volcanic lithic fragments. In lesser amounts, amphiboles were observed in subangular to subrounded crystals (Figure 10e). These components represent 4% of sample PC02, while in the rest of the samples, their abundance is less than 2%. Both components are generally slightly altered or unaltered and decrease in quantity and size towards the top of the section.

The cement in the samples corresponding to the PC section is predominantly calcitic (7% of the total) and is found as pore filling, replacing clasts or as poikilotopic cement (Figure 9b). Occasionally, it is observed as fillings in the vesicles of pumiceous clasts. In sample PC03, argillaceous cement of the pore-filling type predominates (5% of the sample; Figure 9a). Towards the top of the PC section (samples PC04, PC05A and PC05B), local ferruginous cement is observed, surrounding the clasts (Figure 10f). In the samples from the IH profile, argillaceous cement predominates, followed by ferruginous cement, which is found surrounding the clasts and as pore filling.

The analysis using the scanning electron microscope (SEM) was performed on a sample from the Ingeniero Huergo section (IH05), corresponding to a coarse sandstone with parallel lamination and abundant vitreous lithic fragments. In the obtained images, it is possible to differentiate both massive and fibrous-looking shards (Figure 11a) and pumiceous fragments with vesicles of different morphologies (Figure 11b,c). Additionally, clays were identified covering the vesicles in most of the vitreous components (Figure 11c,d). Although the characteristics of the sample did not allow for an exact mineral species determination, The habits mainly correspond to clays of the smectite group and subordinately to illite (Welton 1984).

In the analysis by energy dispersive x-ray spectroscopy (EDS) of the clays covering the vesicles, peaks of Si, O, Al, Na, K, Fe and Mg were observed (Figure 12a). Additionally, the sample generally showed the presence of iron oxides and, to a lesser extent, manganese. These are also associated with peaks of Mg and Ti and can be found concentrated as precipitates on the grains (Figure 12b) and, in the case of iron, also dispersed throughout the sample.

7 | Detrital Zircon U–Pb Geochronology

U–Pb ages analysis on detrital zircons ($n = 68$; see Supporting Information S2) was conducted on a sample collected from the top of the El Palo Formation in the Paso Córdoba area (PPC01-20—39°8′50.70″S; 67°40′26.30″W). The sample consists of a reworked pumice fragment, and its position in the section is detailed in Figure 2. The frequency histogram and relative probability plot show a multimodal pattern in the age distribution, with four main populations observed (Figure 13a). The predominant population consists of Permian–Triassic ages (35%), followed by Jurassic–Cretaceous ages (22%), Devonian–Carboniferous ages (22%) and Paleogene–Neogene ages (13%). Minor peaks of Proterozoic (5%) and Ordovician–Silurian (3%) ages are also distinguished.

Among the younger Neogene ages, a population of three zircons was identified for calculating a maximum depositional age, using the measurement criteria proposed by Dickinson and Gehrels (2009). Based on the data analysis, weighted mean average of the youngest cluster of two or more grains ages that overlap at 1σ uncertainty was the best estimation method for the PPC01-20 sample from the El Palo Formation. The analytical details are provided in the Supporting Information. Using this method, the calculated maximum depositional age is 14.6 ± 1 Ma (1σ; $n = 3$), corresponding to the Middle Miocene (Figure 13b).

8 | Discussion

8.1 | Depositional Model

The facies analysis in this study suggests that the sediments of the Chichinales and El Palo formations were deposited in continental environments with the development of fluvial systems. Regarding the Chichinales Formation, the predominance of fine-grained deposits from floodplain settings (FA1) and the interbedding of isolated single-story channel bodies (FA2) suggest a low-energy fluvial system and the development of floodplain deposits (Figure 14a), which is consistent with the interpretations by Uliana (1979) and Barrio et al. (1989). The recognition of lateral accretion structures in the Bajo Los Menucos area, also described in Hugo and Leanza (2001b), indicates the presence of high-sinuosity channels (Miall 1996), at least in this sector. The presence of palaeosols and iron–manganese nodules indicates periods of stability and seasonal water saturation of the soils (PiPujol and Buurman 1997). These conditions were also recognised by Barrio et al. (1989), who interpreted the existence of strongly seasonal paleoclimates.

For the deposits of the El Palo Formation, Uliana (1979) interpreted the development of an anastomosed fluvial system. While in the past this term was frequently used synonymously with braided systems, it is currently recommended to use it to describe networks of stable channels within vegetated floodplains (Miall 1996, 2014). In the analysis carried out in this study, the predominance of deposits corresponding to FA3 was observed for the El Palo Formation. Based on the presence of

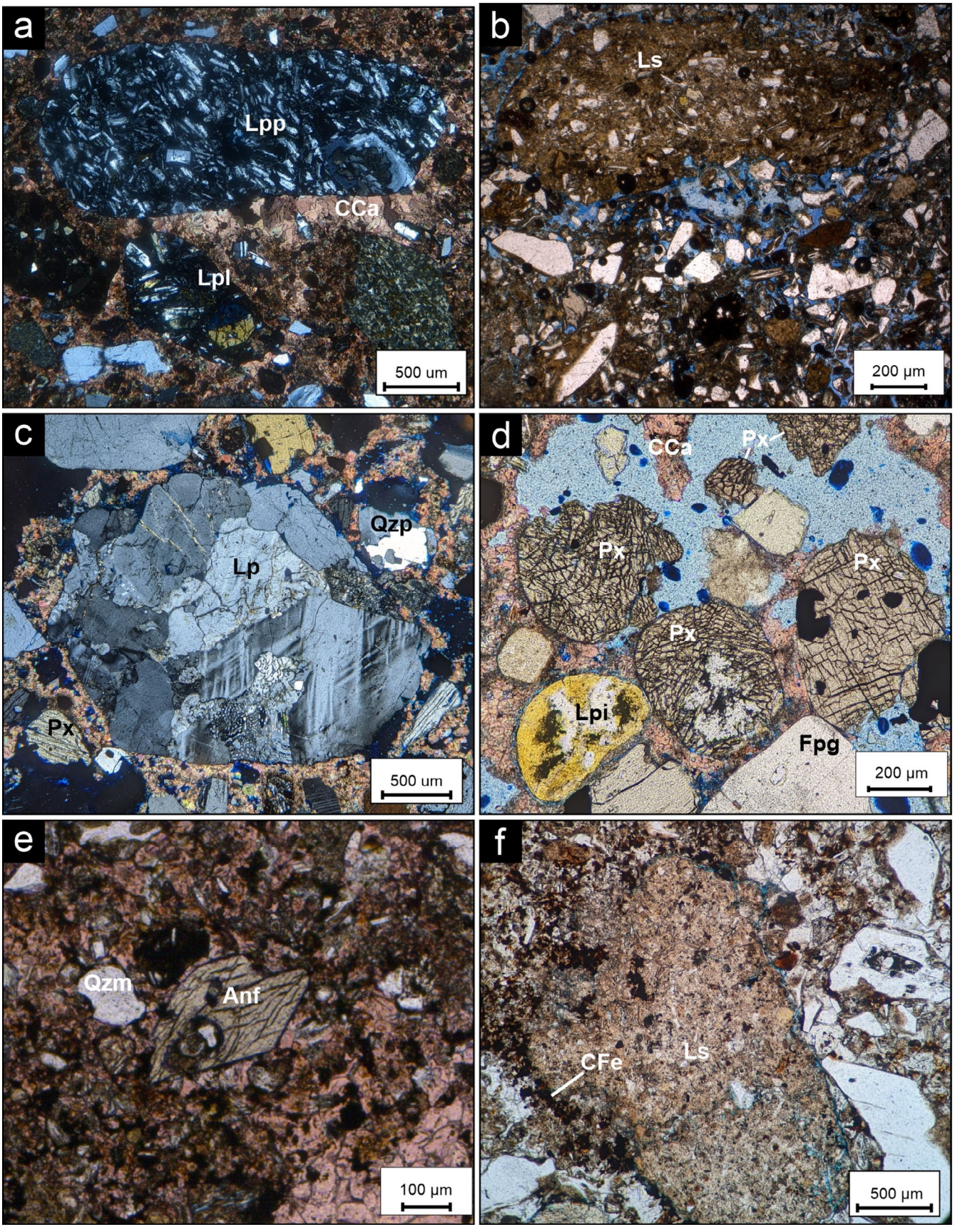

FIGURE 10 | Legend on next page.

FIGURE 10 | (a) Mafic paleovolcanic lithic fragments with pilotaxitic (Lpp) and lathwork (Lpl) textures are observed, surrounded by calcareous cement (CCa). (b) Sedimentary lithic of volcaniclastic composition (Ls). (c) Plutonic lithic fragment (Lp) composed of graphic-textured quartz, alkaline feldspar and plagioclase. Polycrystalline quartz (Qzp) and pyroxene (Px) are also visible. (d) Abundant fractured pyroxenes (Px), pyroclastic lithic fragment (Lpi), plagioclase (Fpg) and calcareous cement (CCa). (e) Amphibole (Anf) in a basal section with two visible cleavage directions. (f) Sedimentary lithic fragment (Ls) with poikilotopic ferruginous cement (CFe).

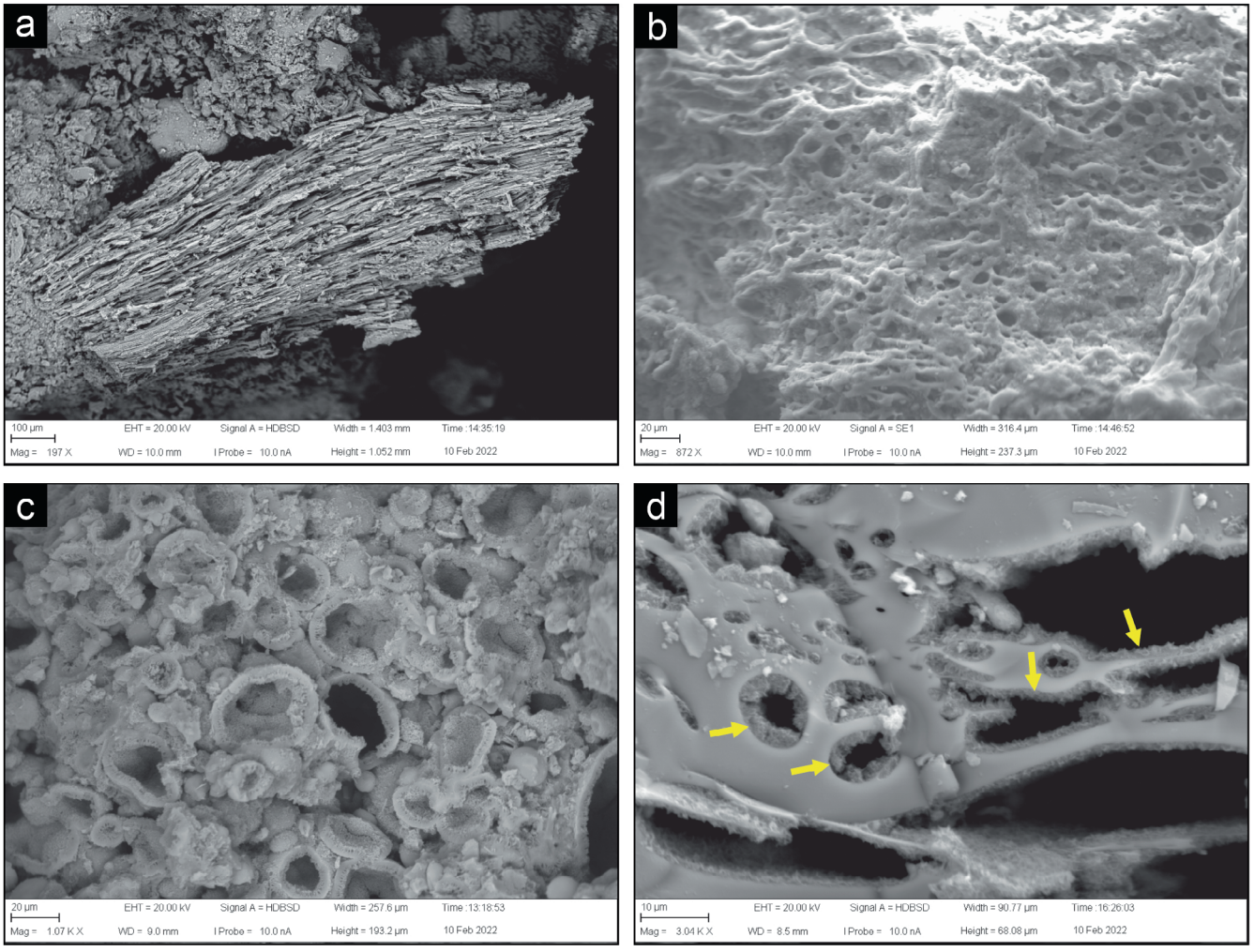

FIGURE 11 | Images of sample IH05 under a scanning electron microscope. (a) Fibrous-looking glass shard; (b, c) vesicles with different morphologies in pumice clasts. (d) Presence of clays covering vesicle walls in a pumice clast, indicated by yellow arrows.

multiepisodic gravelly sandy channelised deposits, limited by erosional surfaces and poor exposure of floodplain deposits, a braided fluvial system with high channel mobility is interpreted for this facies association (Gibling 2006; Figure 14b). The predominance of downstream accretion macroforms, at least in the Mainqué section, indicates the development of low-sinuosity channels in that area (Miall 2014). The FA4 are less represented and were interpreted as sediment gravity flows and sheet-flood deposits, corresponding to high sediment concentrations (Miall 1996). The identification of pyroclastic material in almost all the analysed samples, including individual angular shards and pumice, the occasional presence of mudstone beds with a high proportion of vitreous shards, and the provenance analysis suggest that sedimentation occurred contemporaneously with volcanic activity in the arc. The presence of sediment gravity flows with abundant pyroclastic material is commonly another indicator of direct contributions from large-scale explosive volcanic eruptions to fluvial systems (Smith 1987; Kataoka and Nakajo 2002). However, the presence of pumice fragments with varying degrees of alteration, the mixture of source areas and the low percentage of younger zircons may suggest a delayed environmental signal resulting from the erosion of different volcaniclastic units in the catchment area, rather than constituting synchronous evidence of volcanism.

As mentioned in the Background section, both tectonic and climatic processes played pivotal roles in shaping the Neogene alluvial–fluvial systems of northern Patagonia (Bilmes et al. 2013; Bucher et al. 2020; López et al. 2019, 2024; García Morabito et al. 2021). The interplay of these factors exerted a long-term influence on the sedimentary environments preserved in the Miocene deposits of Northern Patagonia.

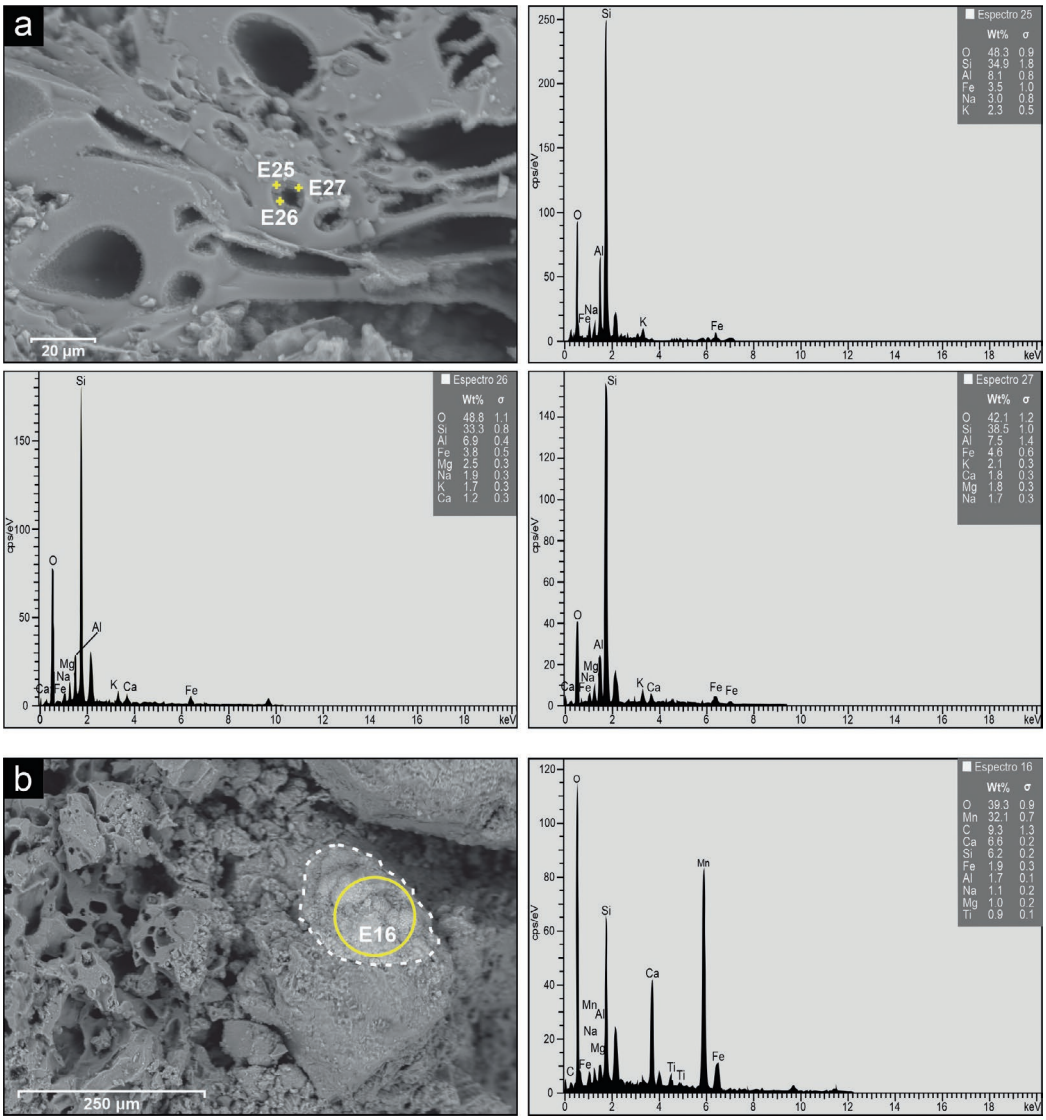

FIGURE 12 | (a) EDS (Energy Dispersive X-ray Spectroscopy) analysis of clays covering the walls of vesicles at three points (E25, E26 and E27). Main peaks are observed for O, Si, Al, Fe, Na, K, Mg and Ca. Yellow crosses indicate the analysed points. (b) EDS analysis of a precipitate in a clast, with high values of manganese. The yellow circle indicates the analysed area.

This dynamic is particularly evident in the sedimentary records of the Chichinales and El Palo formations within the study area. The transition in fluvial dynamics between these units is marked by the presence of palaeosols in the Chichinales Formation and their subsequent absence or limited preservation in the El Palo Formation (Figure 14), as well as evident changes in particle size and composition between these units. This underscores the combined influence of allocyclic factors—tectonics and climate—on the evolution of these depositional systems.

8.2 | Origin, Transport and Depositional Processes of Pumice Fragments

Pumice fragments have unique hydrodynamic characteristics compared to clasts of other compositions, among which their low density stands out, making it easy to initiate and sustain movement in a flow. They are also temporarily buoyant in water when cold and dry (Witham and Sparks 1986; Manville et al. 1998, 2002).

When deposited alongside denser clasts from a stream, pumice fragments tend to be larger in comparison. This phenomenon of hydraulic equivalence between clasts of different sizes and densities has been studied by several authors (Manville et al. 1998, 2002; White et al. 2001; Colombo et al. 2018). The variable density of the pumice clasts depending on their degree of water saturation also constitutes a factor that alters the equivalence with denser material or even with other pumice fragments (White et al. 2001).

Considering the thickness, lateral extent and high proportion of pumice fragments in the El Palo Formation, these fragments likely originated from the reworking of pumice-rich pyroclastic deposits, which were subsequently redeposited in a fluvial context (Kataoka 2003).

The youngest zircons used to calculate the maximum depositional age of 14.6 ± 1 Ma obtained in the El Palo Formation from a pumice fragment show ages very close to those obtained by other authors in volcaniclastic deposits associated

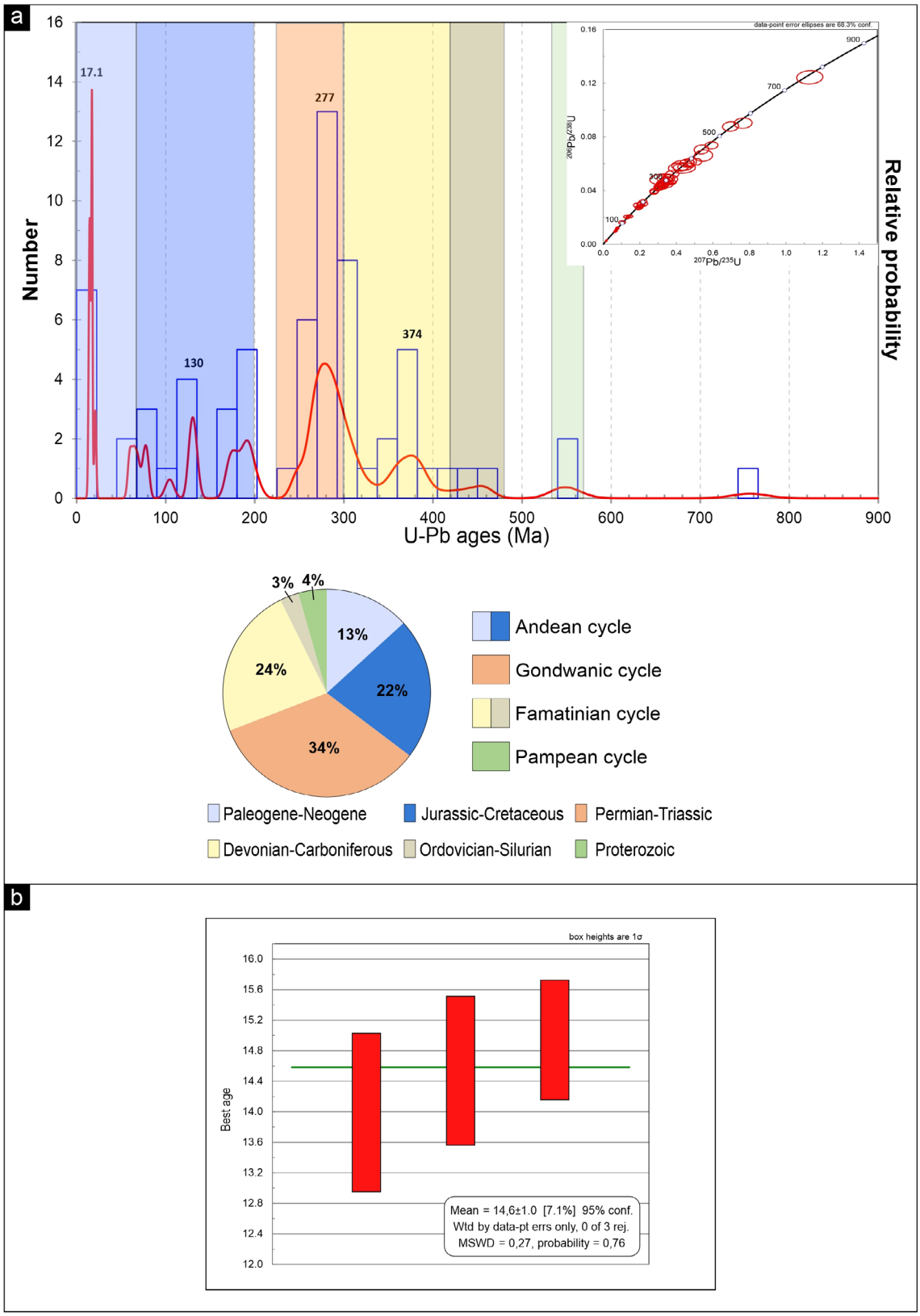

FIGURE 13 | (a) Frequency histogram, relative probability and concordia diagrams for the U–Pb ages of sample PPC01-20 ($n = 68$) and interpreted provenance of detrital zircons. (b) Calculation of the weighted mean using the ages of the three youngest overlapping zircons with a 1σ uncertainty.

with significant Miocene volcanism, mainly outcropping in the Patagonian Broken Foreland zone (Bilmes et al. 2013). These ages range from 15 to 14 Ma and belong to the Pilcaniyeu Member of the Collón Cura Formation (Marshall and Pascual 1977; Rabassa 1975; Mazzoni and Benvenuto 1990; López 2020). González Díaz et al. (1990) also obtained a K/Ar age of 14.1 ± 1 Ma for an ignimbrite in the middle part of the Limay Chico Member of the Caleufú Formation. Studies

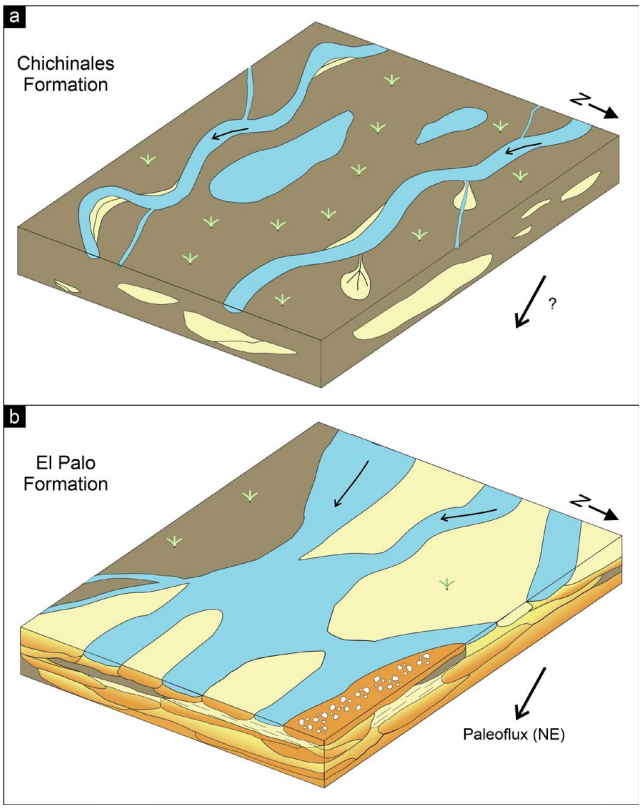

FIGURE 14 | (a) Schematic depositional model interpreted for the Chichinales Formation, composed of a low to moderate energy fluvial system with isolated sandy channels interbedded with floodplain deposits. (b) Schematic model for the El Palo Formation, representing a braided, moderate-to-high energy fluvial system with occasional gravity flow and sheet flow deposits.

conducted in that region have suggested a connection between the drainage systems of the Collón Cura Basin area and those developed in the North Patagonian Basin during the Miocene (Bilmes et al. 2019).

Based on the previous data, together with the absence of primary volcaniclastic deposits and eruptive centres of this style in the study area, the pumice components of the El Palo Formation are interpreted to have originated from the reworking of pumiceous pyroclastic deposits. These pyroclastic deposits were likely generated in the Patagonian Broken Foreland, implying the fluvial transport of the pumice fragments for over 200 km before their deposition. In addition to the example presented in this study, Miocene fluvial deposits with pumice fragments up to 10 cm in size have also been reported eastward of the study area (Escosteguy et al. 2011) and pumiceous psephitic clasts between General Conesa and Viedma (Andreis 1965), both belonging to the Río Negro Formation. These localities are situated over 100 km to the east of the study area and over 300 km from the volcanic arc. While these pumice fragments and those in the study area may not be directly related, they provide additional evidence of the fluvial transport capacity of these large-sized components over long distances within the same basin.

Several studies have analysed volcaniclastic sedimentation in continental environments located over 100 km from the eruptive source (Kataoka et al. 2009 and references cited therein), although few studies have described large-sized pumice in such deposits. Examples of this are presented by Mack et al. (1996) and Kataoka et al. (2003), who mention monomictic pumice conglomerates and sandstones with clasts reaching decimetric sizes, deposited respectively over 400 and 150 km from the eruptive source. Both cases involved the reworking of primary pumice-rich pyroclastic deposits and subsequent fluvial transport, both by high-concentration sediment flows and diluted flows.

Regarding the El Palo Formation, the different types of occurrence and sedimentary structures in the deposits composed of pumice fragments indicate variability in the transport and deposition processes. Monomictic levels or those with a high concentration of pumice fragments suggest rapid transport from the source area in sediment-laden flows, avoiding segregation and mixing with clasts of other compositions (Mack et al. 1996). Beds with a low proportion of pumice clasts in some cases may correspond to locally reworked previous pumice deposits or clasts that remained in the system for a longer period before deposition, allowing mixing with other materials. The presence of more than one level with a high proportion of pumice fragments, vertically separated by several meters, indicates the occurrence of multiple pumice deposition events.

The larger pumice clasts, reaching a size range of 20–30 cm, are commonly found in conglomerate sets with tabular or irregular geometries, internally massive or with diffuse stratification, poorly sorted, and with a high proportion of pumice fragments, sometimes forming monomictic beds (facies Gmm). These characteristics suggest deposition from gravitational sediment flows, possibly hyperconcentrated flows (Miall 1996; Vallance and Iverson 2015). Alternatively, some of the monomictic deposits with poor sorting may represent cluster-type fabrics, where the frictional locking and low hydraulic contrast between small and large pumice clasts result in their joint deposition on the bed during periods of low flow velocity (White et al. 2001; Manville et al. 2002).

Pumice fragments that are part of tractional sedimentary structures must have been transported and deposited by sedimentary processes common to clasts of other compositions, although their low density and hydrodynamic features give them distinctive properties. A particularity of the pumice fragments forming tractive sedimentary structures in the analysed sections is, compared to massive deposits, they present smaller sizes, usually not exceeding lapilli size. This difference in sizes could be associated with several factors. For instance, larger pumice fragments retain their buoyancy for a longer time than smaller ones, remain in motion even at very low flow velocities and, once deposited, are easily remobilised, which hinders their deposition in bed forms (Manville et al. 1998, 2002). Moreover, pumice generally exhibits low resistance to mechanical abrasion due to its high porosity, resulting in significant volume loss associated with clast impacts, which could have reduced their size during transport (Stanley 1978; De Lange 1988). In all cases, it was observed in mixed composition beds that the epiclastic material has a smaller size than the pumice fragments, which was interpreted as a product of hydraulic equivalence between grains of different sizes and densities (Manville et al. 1998, 2002).

8.3 | Age Distribution and Provenance

While the dated sample corresponds to a pumice fragment, due to its reworked nature, the wide range of ages it presents and the low percentage of Miocene ages, it is interpreted that most of the dated zircons are likely detrital zircons that were incorporated into the vesicles and matrix during the pumice transport to the deposition area (Figure 13a). The younger zircons used for interpreting a maximum sedimentation age, on the other hand, could correspond to the volcanic event that generated the pumice (Figure 13b).

Based on the multimodal age pattern obtained, it is possible to interpret different sources for the zircons analysed in sample PPC01-20 (Figure 13a). The oldest ages consist of two minor peaks from the Late Neoproterozoic and Ordovician. Similar-aged outcrops can be found in both the Chadileuvú Block and the North Patagonian Massif (Pankhurst et al. 2006; Chernicoff et al. 2010, 2012). Considering the sample's position and paleocurrent directions, the latter option is more probable. Furthermore, Devonian ages were identified, with a peak at 373 Ma. Ages in the range of 420–350 Ma have been described in igneous and metaigneous rocks of the North Patagonian basement and in plutons of the San Rafael Block (Varela et al. 2005; Cingolani et al. 2005; Pankhurst et al. 2006). The main population of zircons corresponds to Gondwanan ages, with a peak at 277 Ma. This peak possibly represents the magmatism of the Choiyoi Group, which is part of the basement of the Neuquén Basin and is widely distributed in the Andean sector and the North Patagonian Massif (Kay et al. 1989; Sato et al. 2015). Ages postdating the Gondwanan Cycle are interpreted as part of the Andean Cycle, which began in the Middle Triassic (Llambías et al. 2007). Zircons from the Late Triassic to Early Jurassic could be associated with volcanic rocks formed during the initial rifting stage of the Neuquén Basin, while Cretaceous and younger zircons come from the Andean arc (Schiuma and Llambías 2008; Tunik et al. 2010; Balgord 2017; Gómez et al. 2022). Among them, the youngest Neogene ages represent 10% of the ages ($n = 7$). Considering the characteristics of the sample and the ages obtained, a volcanic provenance is interpreted for the latter.

Alternatively, older zircons could have been incorporated into the magma from which pumice derived through crustal assimilation processes (Brown and Smith 2004; Pittari et al. 2008; Cooper et al. 2014; Pack et al. 2016), rather than being of detrital origin. The Palaeozoic and Mesozoic age peaks obtained are consistent with ages documented in the basement of the North Patagonian Massif and North Patagonian Cordillera, as well as with magmatic events associated with the North Patagonian Batholith (Pankhurst et al. 1999; Varela et al. 2005; Aragón et al. 2011).

The significant contribution of volcanic material in the El Palo Formation is evidenced by the abundance of lithic fragments with extrusive textures. The presence of pumice-rich levels, mudstones with high volcaniclastic content and pumiceous or cuspate vitroclasts in almost all the analysed samples indicates an explosive volcanic source. The presence of partially clay-coated vitric components indicates incipient alteration of the glass, possibly due to diagenetic processes (McPhie et al. 1996). As discussed earlier, these components are likely the result of reworking of coeval pyroclastic deposits, derived from the Andean volcanic arc. This is also supported by a geochemistry analysis on a pumice sample from the El Palo Formation in the same study area, carried out by Rodríguez et al. (2023). More than 200 km towards the southwest of this area, primary volcaniclastic deposits with ages similar to the youngest zircons dated in sample PPC01-20 can be found. These deposits, with ages in the range of 15–14 Ma, correspond to the Pilcaniyeu Ignimbrite of the Collón Cura Formation, outcropping in the Patagonian Broken Foreland (Marshall and Pascual 1977; Rabassa 1975; Mazzoni and Benvenuto 1990; López 2020). Additionally, an age of 14 ± 1 Ma was obtained for an ignimbrite in the middle part of the Limay Chico Member of the Caleufú Formation (González Díaz et al. 1990). While it is not possible to directly link these deposits to the volcaniclastic components of the El Palo Formation, they do indicate significant explosive volcanic activity during that time. Additionally, a connection between sediment transfer systems of the mentioned basins and the North Patagonian Basin has been suggested for the Miocene, which could have allowed sediment transport to the study area (Bilmes et al. 2019).

In the El Palo Formation, volcanic lithic fragments with pilotaxic and lathwork textures, as well as zoned plagioclases, are abundant. These components, together with the locally significant presence of pyroxenes and amphiboles (e.g., sample PC02), indicate a source related to intermediate to mafic volcanic rocks. Cenozoic volcanic rocks with such composition are widespread in northern Patagonia, outcropping in the Andean zone, extra-Andean regions, and the North Patagonian Massif (Rapela et al. 1988; Ardolino et al. 1999; Aragón et al. 2011).

Consistent with the predominance of volcanic lithic fragments in the samples, the Dickinson et al. (1983) diagrams show a provenance mostly related to the erosion of a magmatic arc. In the QFL diagram (Figure 8b), a change in sample composition is observed, ranging from the dissected arc field at the base to transitional arc and nondissected arc fields towards the top. In the QmFLt diagram (Figure 8b), the samples plot in the fields of mixing, transitional arc and lithic recycling, from base to top. These patterns are indicative of a change in the source area and correspond to the increase in the proportion of volcaniclastic material observed towards the top of the unit.

8.4 | Correlations

The previous ages assigned to the El Palo Formation are mainly based on the fossil content of mammals. These findings were made outside the study area, in deposits originally attributed to the Río Negro Formation and later assigned to the El Palo Formation by different authors (e.g., Uliana 1979; Hugo and Leanza 2001a; Folguera et al. 2015). Based on fossils found in the valleys of the Colorado and Negro rivers (Pascual et al. 1984), Bajo de Santa Rosa (Scillato Yané et al. 1975), and the Atlantic coast (Pascual and Bondesio 1985; Alberdi et al. 1997), ages corresponding to the Upper Miocene–Lower Pliocene were attributed to the El Palo Formation. Pascual et al. (1984) also suggested a late Lower Miocene age for the sediments of the Río Negro Formation in the Gran Bajo del Gualicho. In the area of the Atlantic coast, the Río Negro Formation also has dates of 6.78 Ma in the lower member based on Sr. isotopic

ratios in bivalves (Del Río et al. 2018) and 4.41 ± 0.5 Ma in the upper member based on fission track dating (Bigazzi et al. 1995; Alberdi et al. 1997).

The correlation between the sedimentary rocks currently included in the El Palo Formation and other units in the region has been discussed by several authors. In the study area, Weber (1964) and De Ferrariis (1966) assigned these deposits to the Río Negro Formation, mainly based on the presence of bluish-coloured sandstones. However, Uliana (1979) considered that this criterion is not sufficient to establish a correlation, as this type of lithology is repeated in several units in northern Patagonia. Moreover, this author mentioned significant differences in lithology, occurrence and topographic position, and therefore defined them as individual units, assigning a younger age to the Río Negro Formation than to the El Palo Formation. In more recent studies, Folguera et al. (2015) also proposed the El Palo Formation as part of a sedimentation cycle preceding the Río Negro Formation, while other authors continued to consider both units as equivalent (e.g., Hugo and Leanza 2001a; Espinoza and Melchor 2021). Additionally, Espinoza and Melchor (2021) correlated the El Palo Formation with the upper part of the El Sauzal Formation, which outcrops to the north of the study area. The ages obtained in this study for the Paso Córdoba area are more consistent with the proposal by Folguera et al. (2015), at least in terms of the stratigraphic position of the El Palo Formation.

Outside the North Patagonian Basin, in depocenters of the Patagonian Broken Foreland located southwest of the study area, Miocene continental deposits are assigned to the Naupa Huen and Collón Cura formations. These formations have been correlated with the lower and upper parts, respectively, of the Chichinales Formation (Uliana 1979; Huyghe et al. 2014). Recently, an age of 20.49 ± 0.05 Ma ($^{40}Ar/^{39}Ar$) was obtained for the latter unit (Rodríguez et al. 2023). Above the Collón Cura Formation, Miocene fluvial deposits corresponding to the Limay Chico Member of the Caleufú Formation were deposited which, prior to the work of González Díaz et al. (1986),

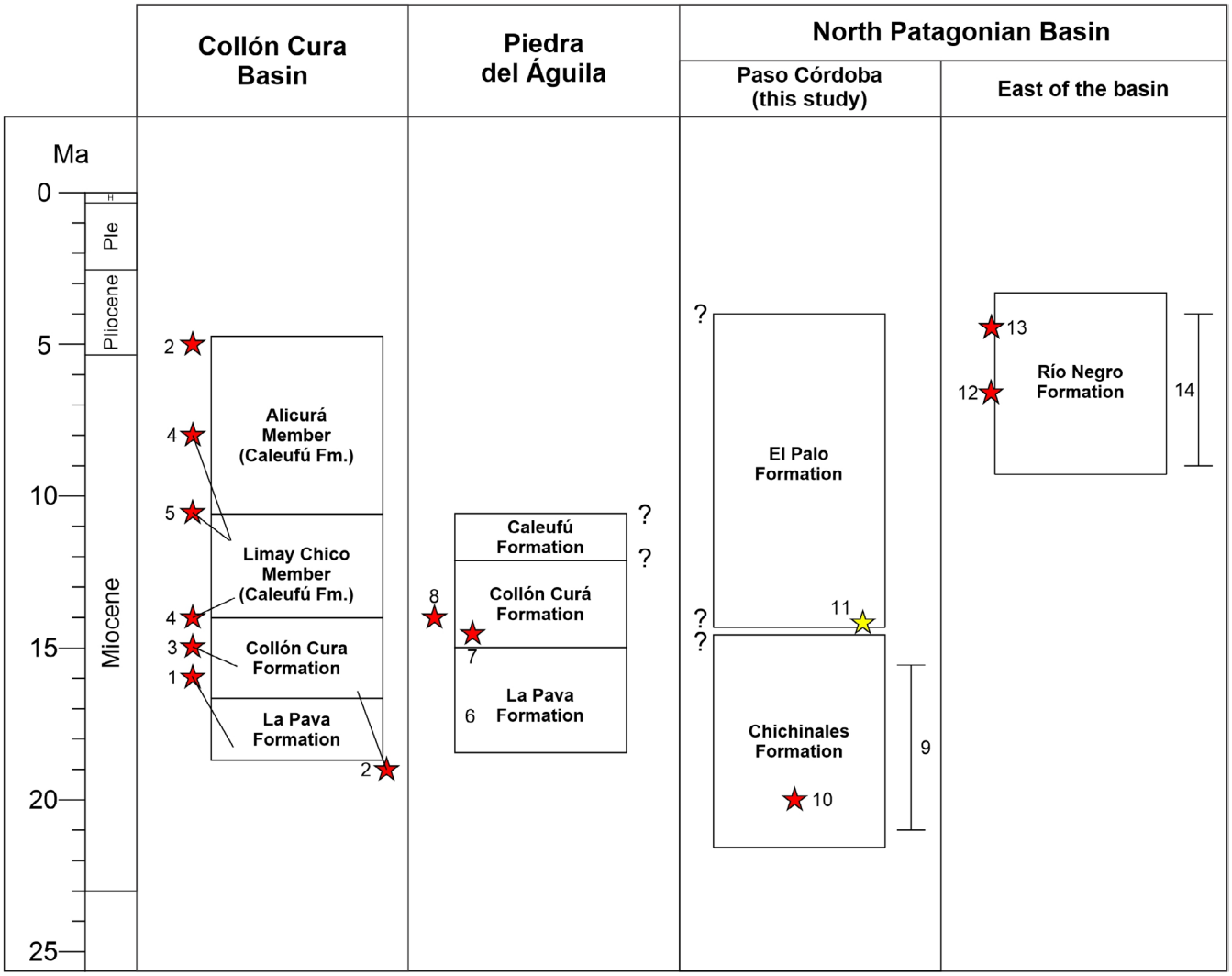

FIGURE 15 | Stratigraphic scheme with radiometric dating of the Miocene sedimentary units in northern Patagonia. (1) Cucchi et al. (1998). (2) Niviere et al. (2019). (3) López (2020). (4) González Díaz et al. (1990). (5) López et al. (2019). (6) D'Elia et al. (2020). (7) Marshall and Pascual (1977). (8) Mazzoni and Benvenuto (1990). (9) SALMAs Colhuehuapense, Santacrucense and Friasense (Pascual et al., 1984; Barrio et al. 1989). (10) Rodríguez et al. (2023), (11) Age obtained in this study. (12) Del Río et al. (2018). (13) Alberdi et al. (1997). (14) Temporal range of the SALMAs Huayqueriense and Montehermosense (Alberdi et al. 1997).

had been assigned to the Río Negro Formation. This member would be equivalent to the 'rionegrense' (González Díaz and Castro Godoy 2008), which in turn was correlated with the El Palo Formation (Uliana 1979). Ages in ignimbrites of 14 ± 1 Ma (K-Ar) in the middle of the unit and 8 ± 2 Ma (K-Ar) and 10.6 ± 0.2 Ma (U–Pb) at the top have been obtained for the Limay Chico Member (González Díaz et al. 1990; López et al. 2019). Moreover, this member has a similar composition to the deposits of the El Palo Formation, with a significant volcaniclastic input and abundant volcanic lithic fragments of basic composition (González Díaz et al. 1986). As mentioned before, there is an evident transition in fluvial dynamics between Chichinales and El Palo Formations, marked by the presence of palaeosols in the former and their subsequent absence or limited preservation in the latter, as well as evident changes in particle size between these units. This is a pattern also observed in Collón Cura Formation and Limay Chico Member to the west. Huyghe et al. (2014) describe outcrops of the Limay Chico Member extending from the Collón Cura area to the Rentería plateau, where it thins and presents minimal thicknesses. These authors present a stratigraphic section in the Paso Córdoba area, where despite describing features similar to the El Palo Formation towards the top of the section, they did not mention this unit and assigned the entire section to deposits of the Chichinales Formation. The Caleufú Formation also includes the Alicurá Member, which González Díaz et al. (1986) correlated with the Bayo Mesa Formation, which outcrops near the study area above the El Palo Formation deposits. Sedimentation in this member was constrained between ~10.6 ± 0.2 and~5 Ma (López 2020).

Despite the different ages proposed for the El Palo Formation and its possible equivalents, no absolute ages in zircons were available for the unit in the study area until now. In this study, the calculation of the maximum depositional age for sample PPC01-20, taken from the top of the El Palo Formation in the Paso Córdoba area, resulted in 14.6 ± 1 Ma (1σ; $n = 3$), corresponding to the Middle Miocene. This age is very close to the ages obtained from primary pyroclastic deposits assigned to the Pilcaniyeu Member in the Collón Cura Formation, mentioned before in Section 8.3, and to the age obtained by González Díaz et al. (1990) for the Limay Chico Member (Figure 15). Although the low percentage of young zircons indicates significant reworking, the characteristics of the deposits and the provenance analysis suggest that coeval volcanic activity was present. The significant difference between the previously assigned age and the one obtained in this study could correspond to different possibilities: (1) the lower temporal limit of the unit could be older than suggested in previous studies, at least in the study area; (2) due to the reworking of volcaniclastic deposits, the pumice sample used for dating could belong to a previous event and was incorporated along with the younger volcaniclastic material in the source area (e.g., Mack et al. 1996) or (3) alternatively, the age could indicate that sedimentation of pumice fragments was not coeval with the volcanic activity evidenced in this unit and that pumice comes from reworking of older deposits.

9 | Conclusions

- The sediments of the Chichinales and El Palo formations analysed in this study were deposited in continental fluvial environments. The deposits of the Chichinales Formation represent a system of moderate to low energy, with extensive development of floodplain in wet conditions and periods of stability with the formation of palaeosols. The El Palo Formation shows a system of moderate-to-high energy, with meandering channels of high mobility and occasional periods of high discharge, represented by sediment gravity flows and sheet-flood deposits. The transition between these units reflects the combined influence of allocyclic factors—tectonic activity and climate variability—on the evolution and characteristics of these depositional systems.
- The pumice fragments observed in the El Palo Formation originate from the reworking of primary volcaniclastic deposits associated with the Andean volcanic arc. The evidence suggests both explosive volcanic activity contemporaneous with sedimentation and the reworking of older volcaniclastic deposits as sources for the pyroclastic components. This explosive volcanic activity may be related to the eruptive events that produced the volcaniclastic deposits of the Collón Cura and/or Caleufú formations, which are exposed in the Patagonian Broken Foreland region.
- The pumice fragments indicate fluvial transport for more than 200 km from the source. These components were transported and deposited by multiple events, both by dilute flows and sediment gravity flows with a high proportion of pumice clasts.
- The provenance analysis of the El Palo Formation samples reveals a predominantly volcanic source, with a change from the samples collected at the base of this unit, which belong to the dissected arc field, to the middle and upper parts that belong to the transitional arc and nondissected arc fields. Considering the sediment composition, zircon ages and measured paleocurrents, the main source would have been from the Andes to the west and the North Patagonian Massif to the south.
- The maximum depositional age obtained in sample PPC01-20, located at the top of the El Palo Formation, is 14.6 ± 1 Ma (1σ; $n = 3$). The significant difference between this age and the younger ages obtained in previous studies could be due to either the lower temporal limit of the unit being older than previously established in the literature, at least in the study area, or the incorporation of pumice fragments from older events into the volcaniclastic sediments of the El Palo Formation.
- Based on the stratigraphic position, composition and age of the deposits, the El Palo Formation could be correlated with the Caleufú Formation, exposed in the region of the Patagonian Broken Foreland.

Acknowledgements

The authors would like to thank Juan Ison for preparing the thin sections; Lic. Martin Parada and Lic. Martin Arce for the SEM images and analysis; and Dr. Diego Pino and Dr. Alejandro Báez for their assistance in the fieldwork and discussion of this work. We also thank Deputy Editor Professor Kerry Gallagher for his support and guidance throughout the editorial process, as well as Dr. Fernando Rey and Dr. Leandro D'Elia for their insightful reviews and constructive comments, which

significantly improved this manuscript. The work was funded by PIP 11220210100275CO (CONICET) and PI 40-A-791 (UNRN). Finally, we want to express our gratitude to the Argentine government for valuing knowledge and investing in science, directly or indirectly contributing to the improvement of people's quality of life.

Conflicts of Interest

The authors declare no conflicts of interest.

Data Availability Statement

The data that support the findings of this study are available in the Supporting Information of this article.

Peer Review

The peer review history for this article is available at https://www.webofscience.com/api/gateway/wos/peer-review/10.1111/bre.70028.

References

Alberdi, M. T., F. P. Bonadonna, and E. Ortiz Jaureguizar. 1997. "Chronological Correlation, Paleoecology and Paleobiography of the Late Cenozoic South American Rionegran Land-Mammal Fauna: A Review." *Revista Espanola de Paleontologia* 12, no. 2: 249–255.

Andreis, R. 1965. "Petrografía y paleocorrientes de la Formación Río Negro." *Revista del Museo de La Plata* 5, no. 36: 245–310.

Aragón, E., A. Castro, J. Díaz-Alvarado, and D. Y. Liu. 2011. "The North Patagonian Batholith at Paso Puyehue (Argentina-Chile). SHRIMP Ages and Compositional Features." *Journal of South American Earth Sciences* 32, no. 4: 547–554.

Ardolino, A., M. Franchi, M. Remesal, and F. Salani. 1999. "La sedimentación y el volcanismo Terciarios en la Patagonia Extraandina: El volcanismo en la Patagonia Extraandina." In *Geología Argentina*, edited by R. Caminos, 579–612. Instituto de Geología y Recursos Minerales.

Balgord, E. A. 2017. "Triassic to Neogene Evolution of the South-Central Andean Arc Determined by Detrital Zircon U-Pb and Hf Analysis of Neuquén Basin Strata, Central Argentina (34-40°S)." *Lithosphere* 9: 453–462.

Barrio, C., A. Carlini, and F. J. Goin. 1989. "Litogénesis y antigüedad de la Formación Chichinales de Paso Córdoba (Río Negro, Argentina)." *Actas 4° Congreso Argentino de Paleontología y Bioestratigrafia* 4: 149–156.

Bigazzi, G., F. P. Bonadonna, G. Leone, and G. Zanchetta. 1995. "Primeros datos geoquímicos y geocronologógicos a partir de algunas cineritas del área bonaerense." In *Evolución biológica durante los últimos cinco millones de años. Un ensayo de correlación con el Mediterráneo occidental*, edited by M. T. Alberdi, G. Leone, and E. P. Tonni, vol. 14, 105–125. Museo Nacional de Ciencias Naturales, CSIC.

Bilmes, A., L. D'Elia, J. Cuitiño, et al. 2019. "The Miocene Foreland Basins of Northern Patagonia: Sediment Transfer Systems from the Southern Andean to the Atlantic Shelf." 25th Latin-American Colloquium of Geosciences, Hamburgo, Alemania, 32–33.

Bilmes, A., L. D'Elia, J. R. Franzese, G. D. Veiga, and M. Hernández. 2013. "Miocene Block Uplift and Basin Formation in the Patagonian Foreland: The Gastre Basin, Argentina." *Tectonophysics* 601: 98–111.

Bridge, J. S. 2003. *Rivers and Floodplains: Forms, Processes and Sedimentary Record*, 491. John Wiley & Sons.

Brown, S. J., and R. T. Smith. 2004. "Crystallisation History and Crustal Inheritance in a Large Silicic Magma System: 206Pb/238U Ion Probe Dating of Zircons from the 1.2 Ma Ongatiti Ignimbrite, Taupo Volcanic Zone." *Journal of Volcanology and Geothermal Research* 135, no. 3: 247–257.

Bryan, S. E., A. G. Cook, J. P. Evans, et al. 2012. "Rapid, Long-Distance Dispersal by Pumice Rafting." *PLoS One* 7: e40583.

Bucher, J., A. Varela, L. D'Elia, et al. 2020. "Multiproxy Paleosol Evidence for a Rain Shadow Effect Linked to Miocene Uplift of the North Patagonian Andes." *Bulletin* 132, no. 7–8: 1603–1614.

Chernicoff, C. J., E. O. Zappettini, J. O. S. Santos, S. Allchurch, and N. J. Mcnaughton. 2010. "The Southern Segment of the Famatinian Magmatic Arc, La Pampa Province, Argentina." *Gondwana Research* 17: 662–675.

Chernicoff, C. J., E. O. Zappettini, J. O. S. Santos, M. C. Godeas, E. Belousova, and N. J. Mcnaughton. 2012. "Identification and Isotopic Studies of Early Cambrian Magmatism (El Carancho Igneous Complex) at the Boundary Between Pampia Terrane and the Río de la Plata Craton, La Pampa Province, Argentina." *Gondwana Research* 21: 378–393.

Cingolani, C. A., E. J. Llambías, M. A. S. Basei, R. Varela, F. Chemale Jr., and P. Abre. 2005. "Grenvillian and Famatinian-Age Igneous Events in the San Rafael Block, Mendoza Province, Argentina: Geochemical and Isotopic Constraints." In *Gondwana 12*, edited by R. J. Pankhurst and G. D. Veiga, 103. Academia Nacional de Ciencias.

Colombo, F., R. Bargalló, L. A. Spalletti, P. Enrique, and I. Queralt. 2018. "Pumice Clasts in Cross-Stratified Basalt-Dominated Sandstones and Conglomerates. Characteristics and Depositional Significance: Huarenchenque Fm. (Neuquén, Argentina)." *Journal of Iberian Geology* 45: 29–46.

Cooper, G. F., C. J. Wilson, B. L. Charlier, J. L. Wooden, and T. R. Ireland. 2014. "Temporal Evolution and Compositional Signatures of Two Supervolcanic Systems Recorded in Zircons from Mangakino Volcanic Centre, New Zealand." *Contributions to Mineralogy and Petrology* 167: 1–23.

Cucchi, R. J., P. Espejo, and R. González. 1998. *Descripción geológica de la Hoja 4169-I Piedra del Águila. 242*, 1–74. Instituto de Geología y Recursos Minerales, Boletín.

De Ferraríis, C. 1966. "Estudio estratigráfico de la Formación Río Negro de la provincia de Buenos. Aires Sus relaciones con la región nordpatagónica." *Anales de la Comisión Cientifica de la Provincia de Buenos Aires* 5, no. 7: 85–116.

De Lange, W. P. 1988. "Wave Climate and Sediment Transport Within Tauranga Harbour, in the Vicinity of Pilot Bay." Tesis Doctoral (inédita). Hamilton, New Zealand, University of Waikato, 189 pp.

Del Río, C. J., S. A. Martínez, J. M. Mcarthur, M. F. Thirlwall, and L. M. Pérez. 2018. "Dating Late Miocene Marine Incursions Across Argentina and Uruguay With Sr-Isotope Stratigraphy." *Journal of South American Earth Sciences* 85: 312–324.

D'Elia, L., A. Bilmes, A. N. Varela, et al. 2020a. "Geochronology, Sedimentology and Paleosol Analysis of a Miocene, Syn-Orogenic, Volcaniclastic Succession (La Pava Formation) in the North Patagonian Foreland: Tectonic, Volcanic and Paleoclimatic Implications." *Journal of South American Earth Sciences* 100: 102555.

Dickinson, W. R., L. S. Beard, G. R. Brakenridge, et al. 1983. "Provenance of North American Phanerozoic Sandstones in Relation to Tectonic Setting." *Geological Society of America Bulletin* 94: 222–235.

Dickinson, W. R., and G. E. Gehrels. 2009. "Use of U-Pb Ages of Detrital Zircons to Infer Maximum Depositional Ages of Strata: A Test Against a Colorado Plateau Database." *Earth and Planetary Science Letters* 288, no. 1–2: 115–125.

Dickson, J. A. D. 1966a. "A Modified Staining Technique for Carbonates in Thin Section." *Nature* 205, no. 4971: 587.

Dickson, J. A. D. 1966b. "Carbonate Identification and Genesis as Revealed by Staining." *Journal of Sedimentary Petrology* 36: 491–505.

Echaurren, A., A. Encinas, L. Sagripanti, et al. 2022. "Fore-To Retroarc Crustal Structure of the North Patagonian Margin: How Is Shortening

Distributed in Andean-Type Orogens?" *Global and Planetary Change* 209: 103734.

Escosteguy, L., M. P. Etcheverría, A. Folguera, M. Franchi, A. Faroux, and P. Getin. 2011. *Hoja geológica 3966-IV, Choele Choel. Provincia de Río Negro*. Instituto de Geología y Recursos Minerales SEGEMAR Boletín 398, 38.

Espinoza, N., and R. N. Melchor. 2021. "Neogene Paleoenvironmental Evolution of the Northern Patagonian Extra-Andean Foreland Basin, Argentina." *Journal of South American Earth Sciences* 112: 103541.

Fisher, R. V., and H. U. Schmincke. 1984. *Pyroclastic Rocks*, 472. Springer-Verlag.

Folguera, A. 2011. "La reactivación neógena de la Pampa Central." Tesis Doctoral, Facultad de Ciencias Exactas y Naturales. Universidad de Buenos Aires (inédita), Buenos Aires, Argentina, 190 pp.

Folguera, A., and M. Zárate. 2009. "La sedimentación neógena continental en el sector extrandino de Argentina central." *Revista de la Asociación Geológica Argentina* 64, no. 4: 692–712.

Folguera, A., M. Zárate, A. Tedesco, F. Dávila, and V. A. Ramos. 2015. "Evolution of the Neogene Andean Foreland Basins of the Southern Pampas and Northern Patagonia (34°-41°S), Argentina." *Journal of South American Earth Sciences* 64: 452–466.

Fossa Mancini, E., E. Feruglio, and J. C. De Yussen Campana. 1938. "Una reunión de geólogos de Y. P. F. y el problema de la terminología estratigráfica." *Boletín de Informaciones Petroleras* 15, no. 171: 1–67.

Franzese, J. R., L. D'Elia, A. Bilmes, et al. 2018. "Evolution of a Patagonian Miocene Intermontane Basin and Its Relationship With the Andean Foreland: Tectono-Stratigraphic Evidences From the Catán Lil Basin, Argentina." *Journal of South American Earth Sciences* 86: 162–175.

Franzese, J. R., L. D'Elia, A. Bilmes, M. Muravchik, and M. Hernández. 2011. "Superposición de cuencas extensionales y contraccionales oligo-miocenas en el retroarco andino norpatagónico: la Cuenca de Aluminé, Neuquén, Argentina." *Andean Geology* 38: 319–334.

Frick, C., and L. E. Kent. 1984. "Drift Pumice in the Indian and South Atlantic Oceans." *Transactions Geological Society of South Africa* 87: 19–33.

García Morabito, E., A. Beltrán-Triviño, C. M. Terrizzano, et al. 2021. "The Influence of Climate on the Dynamics of Mountain Building Within the Northern Patagonian Andes." *Tectonics* 40, no. 2: e2020TC006374.

Garzanti, E. 2019. "Petrographic Classification of Sand and Sandstone." *Earth-Science Reviews* 192: 545–563.

Gibling, M. R. 2006. "Width and Thickness of Fluvial Channel Bodies and Valley Fills in the Geological Record: A Literature Compilation and Classification." *Journal of Sedimentary Research* 76: 731–770.

Gómez, R., M. Tunik, S. Casadio, et al. 2022. "Primeras edades U-Pb en circones detríticos del Grupo Neuquén en el extremo oriental de la Cuenca Neuquina (Paso Córdoba, Río Negro)." *Latin American Journal of Sedimentology and Basin Analysis* 29, no. 2: 67–81.

González Díaz, E. F., and S. Castro Godoy. 2008. "Arroyo Limay chico: un ejemplo de captura fluvial en la cuenca superior del Río Limay (SE de Neuquén)." *Revista de la Asociación Geológica Argentina* 63: 76–83.

González Díaz, E. F., H. A. Ostera, J. C. Riggi, and L. Fauque. 1990. Una propuesta temporal acerca del Miembro Limay Chico (ex "Rionegrense") de la Formación Caleufú, en el valle del rio Collón Cura y adyacencias (SE del Neuquén) XI Congreso Geológico Argentino, San Juan. Actas 2: 243–246.

González Díaz, E. F., J. C. Riggi, and L. Fauque. 1986. "Formación Caleufu (Nov. Nom): reinterpretación de las Formaciones Rio Negro y Alicura, en el área de Collon Cura, sur del Neuquén." *Asociación Geológica Argentina* 41, no. 1–2: 81–105.

Huerta, P., I. Armenteros, and P. G. Silva. 2011. "Large-Scale Architecture in Non-marine Basins: The Response to the Interplay Between Accommodation Space and Sediment Supply." *Sedimentology* 58, no. 7: 1716–1736.

Hugo, C. A., and H. A. Leanza. 2001a. "Hoja Geológica 3969-IV, General Roca, provincias de Río Negro y Neuquén. Programa Nacional de Cartas Geológicas de la República Argentina (escala 1: 250.000)." Servicio Geológico Minero Argentino. Instituto de Geología y Recursos Minerales, Boletín N° 308, Buenos Aires. 106 pp.

Hugo, C. A., and H. A. Leanza. 2001b. "Hoja Geológica 3966-III, Villa Regina, provincia de Río Negro. Programa Nacional de Cartas Geológicas de la República Argentina (escala 1: 250.000)." Servicio Geológico Minero Argentino. Instituto de Geología y Recursos Minerales, Buenos Aires. Boletín N° 309, 72 pp.

Huyghe, D., C. Bonnel, B. Nivière, B. Fasentieux, and Y. Hervouët. 2014. "Neogene Tectonostratigraphic History of the Southern Neuquén Basin (39°–40° 30′ S, Argentina): Implications for Foreland Basin Evolution." *Basin Research* 27, no. 5: 613–635.

Ingersoll, R. V., T. F. Fullard, R. L. Ford, J. P. Grimm, J. D. Pickle, and S. W. Sares. 1984. "The Effect of Grain Size on Detrital Modes; a Test of the Gazzi–Dickinson Point-Counting Method." *Journal of Sedimentary Research* 54: 103–116.

Jutzeler, M., J. Mcphie, S. R. Allen, and A. A. Proussevitch. 2015. "Grain-Size Distribution of Volcaniclastic Rocks 2: Characterizing Grain Size and Hydraulic Sorting." *Journal of Volcanology and Geothermal Research* 301: 191–203.

Kataoka, K. 2003. "Volcaniclastic Remobilization and Resedimentation in Distal Terrestrial Settings in Response to Large-Volume Rhyolitic Eruptions: Examples From the Plio-Pleistocene Volcaniclastic Sediments, Central Japan." *Journal of Geosciences. Osaka City University* 46: 47–65.

Kataoka, K., and T. Nakajo. 2002. "Volcaniclastic Resedimentation in Distal Fluvial Basins Induced by Large-Volume Explosive Volcanism: The Ebisutoge-Fukuda Tephra, PlioPleistocene Boundary, Central Japan." *Sedimentology* 49: 319–334.

Kataoka, K. S., V. Manville, T. Nakajo, and A. Urabe. 2009. "Impacts of Explosive Volcanism on Distal Alluvial Sedimentation: Examples From the Pliocene–Holocene Volcaniclastic Successions of Japan." *Sedimentary Geology* 220, no. 3-4: 306–317. https://doi.org/10.1016/j.sedgeo.2009.04.016.

Kay, S. M., V. A. Ramos, C. Mpodozis, and P. Sruoga. 1989. "Late Paleozoic to Jurassic Silicic Magmatism at the Gondwana Margin: Analogy to Middle Proterozoic in North America?" *Geology* 17: 324–328.

Leddy, J. O., P. J. Ashworth, and J. L. Best. 1993. "Mechanisms of Anabranch Avulsion Within Gravelbed Braided Rivers: Observations From a Scaled Physical Model." In *Braided Rivers*, edited by J. L. Best and C. S. Bristow, 119–127. Geological Society of London.

Llambías, E. J., H. A. Leanza, and O. Carbone. 2007. "Evolución tectono-magmática durante el Pérmico al Jurásico Temprano en la Cordillera del Viento (37°05′ S–37°15′ S): nuevas evidencias geológicas y geoquímicas del inicio de la cuenca Neuquina." *Revista de la Asociación Geológica Argentina* 62, no. 2: 217–235.

López, M. 2020. "Análisis del relleno volcano-sedimentario de la cuenca de Collón Cura y su correlación con el Antepaís Neógeno de los Andes del sur de Neuquén y norte de Río Negro." Tesis Doctoral. (Inédita). Universidad Nacional de La Plata, 208 pp.

López, M., M. García, J. Bucher, et al. 2019. "Structural Evolution and Deformation Events of the Collón Cura Basin: Tectonostratigraphic Implications for the North Patagonian Foreland at the Foot of the Andes." *Journal of South American Earth Sciences* 93: 424–438.

López, M., F. Milanese, L. D'Elia, et al. 2024. "Decoupling External Forcings During the Development of Miocene Fluvial Stratigraphy of the North Patagonian Foreland." *Basin Research* 36: e12821.

Mack, G. H., W. C. Mcintosh, M. R. Leeder, and H. C. Monger. 1996. "Plio-Pleistocene Pumice Floods in the Ancestral Rio Grande, Southern Rio Grande Rift, USA." *Sedimentary Geology* 103: 1–8.

Manville, V., B. Segschneider, and J. D. L. White. 2002. "Hydrodynamic Behaviour of Taupo 1800a Pumice: Implications for the Sedimentology of Remobilised Pyroclastic Deposits." *Sedimentology* 49: 955–976.

Manville, V., J. D. L. White, B. F. Houghton, and C. J. N. Wilson. 1998. "The Saturation Behavior of Pumice and Some Sedimentological Implications." *Sedimentary Geology* 119: 5–16.

Marshall, L. G., and R. Pascual. 1977. "South American Geochronology: Radiometric Time Scale for Middle to Late Tertiary Mamal Bearing Horizons in Patagonia." *Science* 195: 1325–1328.

Mazzoni, M. M., and A. Benvenuto. 1990. "Radiometric Ages of Tertiary Ignimbrites and the Collón Cura Formation, Northwestern Patagonia." XI Congreso Geológico Argentino, San Juan, Actas 2: 87–90.

McPhie, J., M. Doyle, and R. Allen. 1996. *Volcanic Textures*, 198. University of Tasmania.

Miall, A. D. 1996. *The Geology of Fluvial Deposits: Sedimentary Facies, Basin Analysis and Petroleum Geology*, 582. Springer-Verlag, Inc.

Miall, A. D. 2014. *Fluvial Depositional Systems*, 316. Springer.

Nivière, B., D. Huyghe, C. Bonnel, and P. Lacan. 2019. "Neogene Sedimentation and Tectonics in the Collón Curá Basin (Patagonian Andes of Argentina)." *Journal of South American Earth Sciences* 96: 102244.

Ortiz-Jaureguizar, E., and G. A. Cladera. 2006. "Paleoenvironmental Evolution of Southern South America During the Cenozoic." *Journal of Arid Environments* 66, no. 3: 498–532.

Orts, D. L., A. Folguera, A. Encinas, M. Ramos, J. Tobal, and V. A. Ramos. 2012. "Tectonic Development of the North Patagonian Andes and Their Related Miocene Foreland Basin (41 30′ 43 S)." *Tectonics* 31: TC3012.

Pack, B., A. K. Schmitt, J. Roberge, F. G. Tenorio, and B. N. Damiata. 2016. "Zircon Xenocryst Resorption and Magmatic Regrowth at El Chichón Volcano, Chiapas, Mexico." *Journal of Volcanology and Geothermal Research* 311: 170–182.

Pankhurst, R., C. Rapela, C. Fanning, and M. Márquez. 2006. "Gondwanide Continental Collision and the Origin of Patagonia." *Earth-Science Reviews* 76: 235–257.

Pankhurst, R. J., S. D. Weaver, F. Hervé, and P. Larrondo. 1999. "Mesozoic-Cenozoic Evolution of the North Patagonian Batholith in Aysen, Southern Chile." *Journal of the Geological Society* 156, no. 4: 673–694.

Pascual, R., and P. Bondesio. 1985. "Mamíferos terrestres del Mioceno medio tardío de las cuencas de los ríos Colorado y Negro (Argentina). Evolución ambiental." *Ameghiniana* 22, no. 1–2: 133–145.

Pascual, R., P. Bondesio, M. G. Vucetich, G. Scillato Yañe, M. Bond, and E. P. Tonni. 1984. "Vertebrados fósiles cenozoicos." *Relatorio IX Congreso Geológico Argentino* 2, no. 9: 439–461.

PiPujol, M. D., and P. Buurman. 1997. "Dynamics of Iron and Calcium Carbonate Redistribution and Palaeohydrology in Middle Eocene Alluvial Paleosols of the Southeast Ebro Basin Margin (Catalonia, Northeast Spain)." *Palaeogeography, Palaeoclimatology, Palaeoecology* 134: 87–107.

Pittari, A., R. A. F. Cas, J. A. Wolff, H. J. Nichols, P. B. Larson, and J. Martí. 2008. "The Use of Lithic Clast Distributions in Pyroclastic Deposits to Understand Pre–and Syn-Caldera Collapse Processes: A Case Study of the Abrigo Ignimbrite, Tenerife, Canary Islands." *Developments in Volcanology* 10: 97–142.

Rabassa, J. 1975. *Geología de la región de Pilcaniyeu-Comallo, Provincia de Rio Negro, Argentina 17*, 129. Fundación Bariloche, Departamento Recursos Naturales y Energéticos.

Rapela, C. W., L. Spalletti, J. Merodio, and E. Aragón. 1988. "Temporal Evolution and Spatial Variation of Early Tertiary Volcanism in the Patagonian Andes (40°S-42°30′S)." *Journal of South America Earth Sciences* 1: 75–88.

Rodríguez, M. F., A. L. Casa, C. N. Dal Molin, and I. N. Hernando. 2023. *Hoja Geológica 3969-24 General Roca, provincia de Río Negro. Escala 1:100.000*, 107. Servicio Geológico Minero Argentino. Instituto de Geología y Recursos Minerales, Boletín N° 445.

Sato, A. M., E. J. Llambías, M. A. S. Basei, and C. E. Castro. 2015. "Three Stages in the Late Paleozoic to Triassic Magmatism of Southwestern Gondwana, and the Relationships With the Volcanogenic Events in Coeval Basins." *Journal of South American Earth Sciences* 63: 48–69.

Schiuma, M., and E. J. Llambías. 2008. "Nuevas edades del volcanismo Jurásico Inferior de la cuenca Neuquina en la dorsal de Huincul." *Revista de la Asociación Geológica Argentina* 63: 644–652.

Schumm, S. A. 2005. *River Variability and Complexity*, 220. Cambridge University Press.

Scillato Yané, G. J., M. A. Uliana, and R. Pascual. 1975. "Un Megalonchidae (Edentata, Pilosa) del Plioceno de la Provincia de Río Negro (Argentina) su importancia bioestratigráfica y paleogeográfica." *Actas VI Congreso Geológico Argentino* 1: 579–592.

Smith, G. A. 1987. "The Influence of Explosive Volcanism in Fluvial Sedimentation: The Deschutes Formation (Neogene) in Central Oregon." *Journal of Sedimentary Petrology* 57: 613–629.

Stanley, D. J. 1978. "Pumice Gravels in the Rivière Claire, Martinique: Selective Sorting by Fluvial Processes." *Sedimentary Geology* 21: 161–168.

Tunik, M., A. Folguera, M. Naipauer, M. M. Pimentel, and V. A. Ramos. 2010. "Early Uplift and Orogenic Deformation in the Neuquén Basin: Constraints on the Andean Uplift From U–Pb and Hf Isotopic Data of Detrital Zircons." *Tectonophysics* 489, no. 1–4: 258–273.

Turbeville, B. N. 1991. "The Influence of Ephemeral Processes on Pyroclastic Sedimentation in a Rift-Basin, Volcaniclastic-Alluvial Sequence, Espanola Basin, New Mexico." *Sedimentary Geology* 74: 139–155.

Uliana, M. A. 1979. *Geología de la región comprendida entre los ríos Colorado y Negro, provincias del Neuquén y Río Negro. Tesis Doctoral (inédita)*, 117. Universidad Nacional de La Plata.

Vallance, J. W., and R. Iverson. 2015. "Lahars and Their Deposits." In *Encyclopedia of Volcanoes*, edited by H. Sigurdsson, 2da edición ed., 649–664. Academic Press.

Varela, R., M. A. S. Basei, C. A. Cingolani, O. Siga Jr., and C. R. Passarelli. 2005. "El basamento cristalino de los Andes Norpatagónicos en Argentina: geocronología e interpretación tectónica." *Revista Geologica de Chile* 32, no. 2: 167–187.

Weber, E. I. 1964. "Estudio geológico de General Roca (provincia de Río Negro)." Tesis Doctoral Universidad de Buenos Aires, (inédito). Buenos Aires. 149 pp.

Welton, J. E. 1984. *SEM Petrology Atlas*, 47–78. American Association of Petroleum Geologists.

White, J. D. L., V. Manville, C. J. N. Wilson, B. F. Houghton, N. R. Riggs, and M. Ort. 2001. "Settling and Deposition of AD 181 Taupo Pumice in Lacustrine and Associated Environments." *Special Publication of the International Association of Sedimentologists* 30: 141–150.

Witham, A. G., and R. S. J. Sparks. 1986. "Pumice." *Bulletin of Volcanology* 48: 209–223.

Supporting Information

Additional supporting information can be found online in the Supporting Information section.